SECURITY INFORMATION

CONFIDENTIAL

Copy 241

RM A51J11

53-28-38

NACA RM A51J11

TECH LIBRARY KAFB, NM
0142915

NACA

RESEARCH MEMORANDUM

THE EFFECTS AT TRANSONIC SPEEDS OF THICKENING THE TRAILING EDGE OF A WING WITH A 4-PERCENT-THICK CIRCULAR-ARC AIRFOIL

By Joseph W. Cleary and George L. Stevens

Ames Aeronautical Laboratory
Moffett Field, Calif.

Classification cancelled (or changed to Unclassified)
By Authority NASA Tech Pub Announcement
(OFFICER AUTHORIZED TO CHANGE)
By 71 7 Oct 54
(GRADE OF OFFICER MAKING CHANGE)
11 Apr 61
DATE

CLASSIFIED DOCUMENT

This material contains information affecting the National Defense of the United States within the meaning of the espionage laws, Title 18, U.S.C., Secs. 793 and 794, the transmission or revelation of which in any manner to an unauthorized person is prohibited by law.

NATIONAL ADVISORY COMMITTEE
FOR AERONAUTICS

WASHINGTON
December 11, 1951

CONFIDENTIAL

3/9.98/3

TECH LIBRARY KAFB, NM
0142915

NATIONAL ADVISORY COMMITTEE FOR AERONAUTICS

RESEARCH MEMORANDUM

THE EFFECTS AT TRANSONIC SPEEDS OF THICKENING THE TRAILING EDGE OF A WING WITH A 4-PERCENT-THICK CIRCULAR-ARC AIRFOIL

By Joseph W. Cleary and George L. Stevens

SUMMARY

The effects of a systematic variation of trailing-edge thickness of a symmetrical, circular-arc airfoil on the aerodynamic force, moment, base-pressure, and wake fluctuations have been investigated using the transonic-bump testing technique. An investigation of the effects of one boattail modification was also made. The airfoils were 4 percent thick, of rectangular plan form, and of aspect ratio 4. The testing covered a Mach number range from 0.60 to 1.10 with a corresponding Reynolds number range from about 1.7 to 2.2 million.

At subsonic Mach numbers, the results show a beneficial effect on the lift-drag ratios with no measurable increase in minimum drag coefficient for a trailing-edge thickness equal to 0.3 of the airfoil thickness. Higher lift-curve slopes were observed in the transonic Mach number range for all the blunt-trailing-edge airfoils as compared to the sharp-edged airfoil and higher maximum lift coefficients were noted at 0.6 Mach number. Surface roughness appeared to have a significant effect on the pitching-moment characteristics of the circular-arc and boattailed airfoils, particularly at high subsonic Mach numbers. Base-pressure coefficients for the blunt-trailing-edge airfoils increased from root to tip. Increasing the trailing-edge thickness generally caused a decrease of base-pressure coefficient.

Surveys in the wakes of the airfoils indicated approximately the same level of wake fluctuations for trailing-edge thicknesses of 0 and 0.3 of the airfoil thickness, but indicated marked increases in wake fluctuations for trailing-edge thicknesses of 0.6 and 1.0.

PERMANENT RECORD

INTRODUCTION

At supersonic Mach numbers, the airfoil section having minimum drag for a prescribed structural strength or stiffness may have a blunt trailing edge, as has been shown through theoretical considerations by Chapman in reference 1. The two-dimensional characteristics of such airfoils of moderate thickness as compared with a more conventional airfoil having a sharp trailing edge have been investigated experimentally at subsonic Mach numbers (reference 2). Although the results of that investigation indicated higher minimum drag for the blunt-trailing-edge airfoil, gains in maximum lift were observed and the lift-curve slope increased at Mach numbers where the lift-curve slope decreased for the sharp-trailing-edge airfoil. Thus, it would seem that blunt-trailing-edge airfoils may be of some practical value at both subsonic and supersonic Mach numbers.

The present investigation was undertaken to evaluate the effect of an increase in trailing-edge thickness on the aerodynamic characteristics of a thin three-dimensional wing in the transonic Mach number range. For this investigation, the thick trailing-edge airfoils were formed by building up the trailing edge to the desired thickness and then fairing to the original airfoil by straight lines. The forward portion of the circular-arc section remained intact and the resulting airfoil was not one of the optimum sections derived in reference 1.

NOTATION

C_D drag coefficient $\left(\frac{\text{twice semispan drag}}{qS}\right)$

C_L lift coefficient $\left(\frac{\text{twice semispan lift}}{qS}\right)$

C_m pitching-moment coefficient, referred to 0.25 $\bar{c}$ $\left(\frac{\text{twice semispan pitching moment}}{qS\bar{c}}\right)$

ΔH amplitude of total-pressure fluctuation, pounds per square foot

$\frac{L}{D}$ lift-drag ratio

$\left(\frac{L}{D}\right)_{max}$	maximum lift–drag ratio
M	Mach number
M_L	local Mach number
P_b	base–pressure coefficient $\left(\frac{p_b - p}{q}\right)$
R	Reynolds number based on mean aerodynamic chord
S	total wing area (twice wing area of semispan model), square feet
V	velocity, feet per second
b	twice span of semispan model, feet
c	local wing chord, feet
$\bar{c}$	mean aerodynamic chord $\left(\frac{\int_0^{b/2} c^2 dy}{\int_0^{b/2} c\, dy}\right)$, feet
h	trailing–edge thickness, feet
p	free–stream static pressure, pounds per square foot
p_b	base pressure, pounds per square foot
q	free–stream dynamic pressure $\left(\frac{1}{2}\rho V^2\right)$, pounds per square foot
t	maximum wing thickness, feet
y	spanwise distance from plane of symmetry, feet
$\frac{t}{c}$	airfoil thickness ratio
α	angle of attack, degrees
ρ	air density, slugs per cubic foot

$\frac{dC_L}{d\alpha}$ slope of lift curve, per degree

a.c. aerodynamic-center position, percent of $\bar{c}$

APPARATUS AND MODELS

The tests were conducted in the Ames 16-foot high-speed wind tunnel. The bump testing technique, as described in reference 3, was employed to extend the test Mach number into the supersonic range. The models were cantilever-mounted on an electrical strain-gage balance permitting simultaneous measurements of lift, drag, and pitching moment. Figure 1 shows typical model installations on the transonic bump.

The models were rectangular airfoils having an effective aspect ratio of 4, as illustrated in figure 2. The models were made of steel. End plates were mounted near the root to reduce the flow leakage through the bump. The sections of the blunt-trailing-edge airfoils were derived from a symmetrical circular-arc section by building up the trailing edge to the desired thickness and then fairing to the original airfoil section by straight lines as illustrated in figure 3. Thus the blunt-trailing-edge airfoils retained the 4-percent maximum thickness of the basic circular-arc section and the forward portion remained intact. The airfoils had trailing-edge thicknesses of 0, 0.3, 0.6, and 1.0 times the maximum thickness.

One airfoil was tested which had a boattail trailing edge. Its section was formed by modifying the airfoil with a 1.0 trailing-edge-thickness ratio by chamfering the trailing edge to 0.6 thickness from 0.95 chord to the trailing edge. (See fig. 3.)

Base pressures were measured by means of an orifice at each of four spanwise stations along the blunt trailing edges. These spanwise stations were at 25, 37.5, 62.5, and 87.5 percent of the wing semi-span. A mercury manometer was used to measure the pressures. Wake total-pressure fluctuations were measured by means of quick-response pressure cells mounted on probes one chord length behind the wing trailing edge. These probes measured fluctuating pressures at three points in the wakes as shown in figure 1. The electrical impulses from these cells were amplified with a carrier-current amplifier and recorded on an oscillograph.

TESTS

Measurements made during the tests consisted of lift, drag, pitching moment, base pressures, and fluctuations of total pressures in the wakes of the airfoils.

Tests with surface roughness on each airfoil were made to evaluate its effect on the force and moment characteristics. The surface roughness consisted of No. 60 carborundum grains lightly sprayed on a bonding agent on the upper and lower surfaces from the leading edge to 0.10 chord.

The tests covered a Mach number range from 0.60 to 1.10. Since the flow deflection angle at the leading edge of the airfoils was about 4.5° the leading-edge shock wave never became attached. Thus the flow field about the model was transonic for the highest Mach number of the test. For the Mach number range of the tests, the Reynolds number varied from about 1.7 million to 2.2 million as shown in figure 4. The angle-of-attack range extended from about −6° to +16° but at the higher Mach numbers it was limited by the model strength to lower values.

CORRECTIONS

A tare of 0.0022 was subtracted from the drag coefficient to take into account the effects of the end plate and the drag was corrected for the interaction of the balance force and moment components. Blockage and tunnel-wall interference effects were assumed negligible since the models were small with respect to the flow field. The indicated test Mach numbers were evaluated from the tunnel calibration for the bump and represent an average of the Mach numbers over the region occupied by the model. Typical Mach number contours are illustrated in figure 5. The data have been corrected for flow inclination which was found to exist over the bump. The effects of flow curvature were not investigated.

RESULTS AND DISCUSSION

Effects of a Systematic Variation of the Trailing-Edge Thickness

The lift, drag, and pitching-moment characteristics of the airfoils are presented in figures 6, 7, 8, and 9. The data are presented for the models with and without surface roughness. For the Reynolds

number range of these tests it is believed that laminar flow was maintained over a large part of the smooth wing surfaces. When surface roughness was employed, it is probable that most of the boundary layer was turbulent. The force and moment data are summarized in figures 10, 11, and 12 for the smooth models. Base-pressure data are presented in figures 13, 14, and 15.

Lift.- An examination of figure 10 shows that for a trailing-edge thickness of 0 the lift-curve slope increased gradually with increasing Mach number and then decreased as supersonic Mach numbers were attained. The effect on the lift-curve slope of increasing the trailing-edge thickness was small at low subsonic Mach numbers but as the Mach number was increased, the lift-curve slopes of the blunt-trailing-edge airfoils increased more rapidly than for the circular-arc airfoil. For trailing-edge thicknesses of 0.3 and 0.6, maximum slopes were reached at 0.94 Mach number, but with 1.0 trailing-edge thickness a maximum was attained at about 0.98 Mach number. At high subsonic Mach numbers, relatively large lift-curve slopes have been attained by 10-percent-thick circular-arc airfoils having blunt trailing edges (reference 2) and by a 12-percent-thick wedge (reference 4). The results of reference 4 also show that at high subsonic Mach numbers the lift-curve slope of a conventional airfoil decreased; whereas that of the wedge airfoil of the same thickness continued to increase. In the present case, a comparison of the lift-curve slopes of an NACA 63A004 airfoil of the same plan form and aspect ratio (reference 5) with those of the 0.3 and 0.6 blunt-trailing-edge airfoils of circular-arc origin shows similar values of lift-curve slope in the transonic Mach number range. Thus it appears that while increases in lift-curve slope can be expected by increasing the trailing-edge thickness of circular-arc airfoils, the marked improvement in lift-curve slope of blunt-trailing-edge airfoils over conventional airfoils indicated by references 2 and 4 would not occur in the transonic range for airfoil thicknesses of the order of 4 percent. The effect of increasing the trailing-edge thickness of conventional airfoils was not considered in the present investigation but the results of reference 6 show that for a 10-percent-thick conventional airfoil, increasing the trailing-edge thickness increases the lift-curve slope.

Although a sufficiently high angle of attack was not reached at the higher Mach numbers to show the effect of trailing-edge thickness on maximum lift coefficient, the data do indicate progressively higher maximum lift coefficients as the trailing-edge thickness was increased at 0.60 Mach number. The effect of surface roughness on the lift characteristics appeared practically negligible except for slightly lower maximum lift coefficients for the various airfoils at 0.60 Mach number.

Pitching moment.- At a lift coefficient of 0.1, increasing the trailing-edge thickness appeared to cause a slight rearward movement of the aerodynamic center but the variation of aerodynamic center with Mach number was similar for all trailing-edge thicknesses (fig. 10). The abrupt rearward movement of the aerodynamic center as supersonic Mach numbers were approached was of the order of 10 to 12 percent of the mean aerodynamic chord for all trailing-edge thicknesses. In general, the effect of surface roughness on the pitching-moment characteristics was of minor importance for all trailing-edge thicknesses except 0 (circular-arc section). For this exception, surface roughness appeared to reduce the nonlinearities for pitching-moment coefficient that occurred near zero lift at subsonic Mach numbers. Thus it seems that surface roughness and, therefore, the type of boundary-layer flow altered the pressure distribution in such a way as to have little effect on the lift but a noticeable effect on the pitching moment. It is known from reference 7 that for a slightly thicker circular-arc airfoil at zero angle of attack the type of boundary layer had a significant effect on the local Mach number distribution at Mach numbers above the critical, but had an unimportant effect for Mach numbers less than the critical. Similarly, the results of the present investigation show that the effect of surface roughness on the pitching moment was largest at high subsonic Mach numbers.

Drag.- The variation of drag coefficient with Mach number shown in figure 11 illustrates the relative changes in drag that can be attributed to increasing the trailing-edge thickness. The data indicate that the minimum drag (at zero lift) of the 0.3 blunt-trailing-edge airfoil was about the same as that of the circular-arc airfoil. However, at lift coefficients of 0.2 and 0.4 lower drags were measured with the 0.3 blunt-trailing-edge airfoil. Similarly, increasing the trailing-edge thickness reduced the drag rise due to lift as compared with the sharp-trailing-edge airfoil.

At lift coefficients from 0 to 0.4, the transonic increase in drag coefficient began at or above a Mach number of about 0.90 for all trailing-edge thicknesses. The minimum drag coefficient (at zero lift) at slightly supersonic Mach numbers was of the order of three times the low-speed drag coefficient for the circular-arc airfoil and two and one-half times the low-speed drag coefficient for a trailing-edge thickness of 0.60. An examination of the drag data (figs. 6(b), 7(b), 8(b), and 9(b)) shows that surface roughness increased the drag for all trailing-edge thicknesses.

Lift-drag ratio.- The results shown in figure 12 indicate higher lift-drag ratios at subsonic Mach numbers with a trailing-edge thickness of 0.3 than with a thickness of 0. Further increase in trailing-edge thickness reduced the lift-drag ratio except at lift coefficients above about 0.65 at 0.60 Mach number. At supersonic Mach numbers, the

data indicate approximately the same values of lift-drag ratio for trailing-edge thicknesses of 0 and 0.30 and slightly lower values for trailing-edge thicknesses of 0.60 and 1.00. The variation of maximum lift-drag ratio with Mach number is shown in figure 10.

Base pressures.- Base pressures indicate trends which are reflected in the drag data. The increase noted in minimum drag with increasing trailing-edge thickness and with increasing Mach number parallels the trend of decreasing pressure coefficient on the base of the blunt trailing edge as shown in figures 13 and 14.

At subcritical speeds, the pressure coefficients on the bases of the blunt-trailing-edge airfoils were considerably lower than the pressures which would normally occur on the rear portions of a sharp-trailing-edge airfoil; hence, the pressure drags of the blunt airfoils would be expected to be higher than the pressure drag of the circular-arc airfoil.

As the free-stream Mach number and also the Reynolds number was increased through the transonic range, a decrease in base-pressure coefficient occurred at speeds approximately corresponding to the drag-divergence Mach number. This trend is shown in figure 14 for the innermost base-pressure measuring station. This decrease probably results when a supersonic expansion occurs around the sharp corner of the blunt trailing edge. The magnitude of this expansion is determined by the shape of the wake and is sufficient to result in a low pressure which was about 40 percent of the free-stream static pressure for the blunt trailing edge with a thickness ratio of 1.0. With increasing Mach number, the base-pressure coefficients increased and the base pressure was approximately 40 percent of the free-stream static pressure up to the highest speeds of the test for this airfoil.

A spanwise gradient of base pressure was found to exist as indicated in figure 15. This gradient, with increasing pressure from root to tip, could be partially due to the velocity gradient over the bump normal to the bump surface; however, this variation was not as large as the spanwise gradient of base pressure.

The variation of base-pressure coefficient with angle of attack for the smooth airfoils with various trailing-edge thicknesses and at the different spanwise stations is shown in figure 13(a). At low subsonic speeds the minimum base-pressure coefficient occurred at zero angle of attack. At transonic speeds the trends indicated essentially a constant base-pressure coefficient with changing angle of attack.

The effect of surface roughness on the base pressure is shown by a comparison of figures 13(a) and 13(b). In general, the addition of surface roughness caused the base-pressure trends to be more consistent.

Comparing the rough condition with the smooth condition indicates that roughness increased the base pressure and delayed the negative peak of base-pressure coefficients at transonic speeds to a higher Mach number. These trends are shown in figure 14. The minimum drag was higher for the airfoils with surface roughness, indicating that any decrease of base drag by the addition of surface roughness was more than canceled by increased friction drag.

Investigation of a Boattailed Trailing Edge

Figure 16 presents the lift, drag, and pitching-moment characteristics of a boattailed airfoil formed by chamfering the trailing edge of the airfoil having 1.0 trailing-edge thickness. (See fig. 3.) The results without surface roughness are summarized in figures 17 and 18 and are compared with those of the airfoil having 1.0 trailing-edge thickness.

It is apparent from figure 17 that boattailing the airfoil increased the lift-curve slope in the transonic Mach number range. For a lift coefficient of 0.1, the change in the aerodynamic center of the boattailed airfoil in the transonic Mach number range was about the same as that for the airfoil having 1.0 trailing-edge thickness but the variation with Mach number was less abrupt as supersonic Mach numbers were approached. A comparison of figure 16 with figure 9 indicates that boattailing the airfoil made the variation of pitching-moment coefficient with lift coefficient more nonlinear for Mach numbers from about 0.70 to 0.90. However, adding surface roughness to the boattailed airfoil made the pitching-moment curves more linear for these Mach numbers.

Figure 18 shows that boattailing the airfoil reduced the minimum drag coefficient significantly but at lift coefficients of 0.2 and 0.4 a smaller reduction in drag coefficient was realized. Thus, only slightly higher maximum lift-to-drag ratios were obtained for the boattailed airfoil as shown in figure 17.

Wake Fluctuation Characteristics

Measurements were made of the total-pressure fluctuations in the wake of the test models since it is possible that these measurements will give an indication of the buffeting characteristics of the blunt-trailing-edge airfoils. Unpublished data obtained by this method yield a buffet boundary which agrees well with the buffet boundary obtained by the accepted method using an accelerometer at the airplane center of gravity.

The wake fluctuations are presented in figure 19 which shows the maximum total-pressure fluctuation divided by free-stream dynamic pressure $\left(\frac{\Delta H}{q}\right)$ as a function of Mach number for the various trailing-edge thicknesses. The maximum total-pressure fluctuation shown in this figure is the maximum picked up by the three probes between the angles of attack of -1° and $+6^\circ$. This method of presentation is used since the pressure fluctuations were random and showed no consistent variation with angle of attack. Limitations of this method are: (1) the pickup probes were stationary and were not necessarily in the position to pick up the maximum wake total-pressure fluctuation; and (2) insufficient data were obtained to make a statistical analysis of the variation of wake fluctuation with angle of attack.

At low speeds (M = 0.60) the wake total-pressure fluctuations increased markedly with increasing trailing-edge thickness. The disturbances set up in the wake were probably sufficiently strong to cause an unsteady circulation to be established around the airfoil, resulting in unsteady forces and, hence, some buffeting.

Investigation of figure 19 shows that the wake fluctuations behind the airfoils having 0 and 0.3 trailing-edge thicknesses were relatively small at low speeds, increased gradually to a peak of 0.25q at a Mach number of 0.90, and then decreased slightly. The wake fluctuations behind the airfoil with 0.6 trailing-edge thickness remained practically constant up to 0.90 Mach number and then increased sharply. The airfoil having a trailing-edge thickness of 1.0 had a wake fluctuation of 0.69q at 0.60 Mach number, decreased to a minimum of 0.31q at 0.92 Mach number, and then increased sharply again as the speed was further increased.

In general, the blunt-trailing-edge airfoils had larger wake fluctuations than the basic circular-arc airfoil and it also appears from this test (see fig. 20) that increasing the trailing-edge thickness above 0.40 of the maximum thickness results in relatively large wake total-pressure fluctuations even at low speeds and hence increases the possibility of buffeting.

The effect of boattailing the blunt trailing edge was to decrease the amplitude of the wake total-pressure fluctuation as compared with the amplitude behind the 1.0 blunt-trailing-edge airfoil at most speeds and also indicated lower amplitudes at Mach numbers greater than 0.90 as compared with the 0.6 blunt-trailing-edge airfoil. Boattailing appears to offer a practical means of reducing the total-pressure fluctuations in the wake and hence the possibility of buffeting of blunt-trailing-edge airfoils.

CONCLUDING REMARKS

Transonic wind-tunnel tests of a series of 4-percent-thick biconvex airfoils with varying amounts of trailing-edge thickness showed an increase of the lift-drag ratios with no measurable increase in minimum drag coefficient for a trailing-edge thickness of 0.3 of the maximum airfoil thickness. Higher lift-curve slopes were observed in the transonic Mach number range for all the blunt-trailing-edge airfoils as compared to the circular-arc airfoil and higher maximum lift coefficients were noted at 0.6 Mach number. Surface roughness had a significant effect on the pitching-moment characteristics of the circular-arc and boattailed airfoils, particularly at high subsonic Mach numbers. Increasing base pressure from root to tip was observed for all the blunt-trailing-edge airfoils, with a progressive decrease in base pressures as the trailing-edge thickness was increased. Surveys in the wake of the airfoils indicated approximately the same level of wake fluctuations for trailing-edge thicknesses of 0 and 0.3 but marked increases in wake fluctuations for trailing-edge thicknesses of 0.6 and 1.0.

Ames Aeronautical Laboratory,
National Advisory Committee for Aeronautics,
Moffett Field, Calif.

REFERENCES

1. Chapman, Dean R.: Airfoil Profiles for Minimum Pressure Drag at Supersonic Velocities – General Analysis With Application to Linearized Supersonic Flow. NACA TN 2264, 1951.

2. Summers, James L., and Page, William A.: Lift and Moment Characteristics at Subsonic Mach Numbers of Four 10-Percent-Thick Airfoil Sections of Varying Trailing-Edge Thickness. NACA RM A50J09, 1950.

3. Axelson, John A., and Taylor, Robert A.: Preliminary Investigation of the Transonic Characteristics of an NACA Submerged Inlet. NACA RM A50C13, 1950.

4. Eggers, A. J., Jr.: Aerodynamic Characteristics at Subcritical and Supercritical Mach Numbers of Two Airfoil Sections Having Sharp Leading Edges and Extreme Rearward Positions of Maximum Thickness. NACA RM A7C10, 1947.

5. Nelson, Warren H., and McDevitt, John B.: The Transonic Characteristics of 17 Rectangular, Symmetrical Wing Models of Varying Aspect Ratio and Thickness. NACA RM A51A12, 1951.

6. Hemenover, Albert D., and Graham, Donald J.: Influence of Airfoil Trailing-Edge Angle and Trailing-Edge-Thickness Variation on the Effectiveness of a Plain Flap at High Subsonic Mach Numbers. NACA RM A51C12a, 1951.

7. Liepmann, Hans Wolfgang, Askenas, Harry, and Cole, Julian D.: Experiments in Transonic Flow. U.S. Air Force Technical Report No. 5667, Feb. 9, 1948.

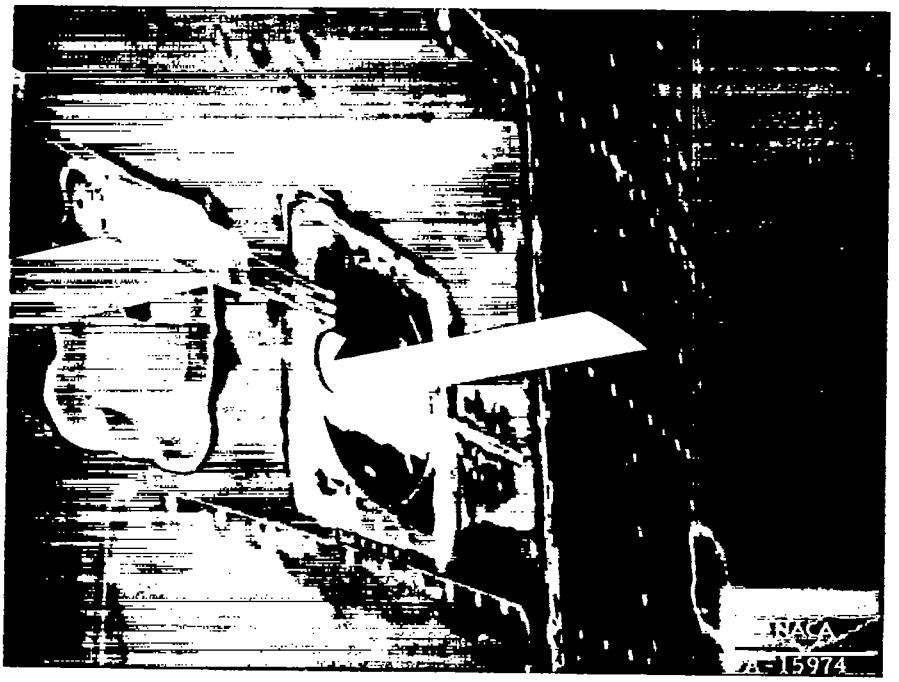

Figure 1.- Typical model mounted on the transonic bump.

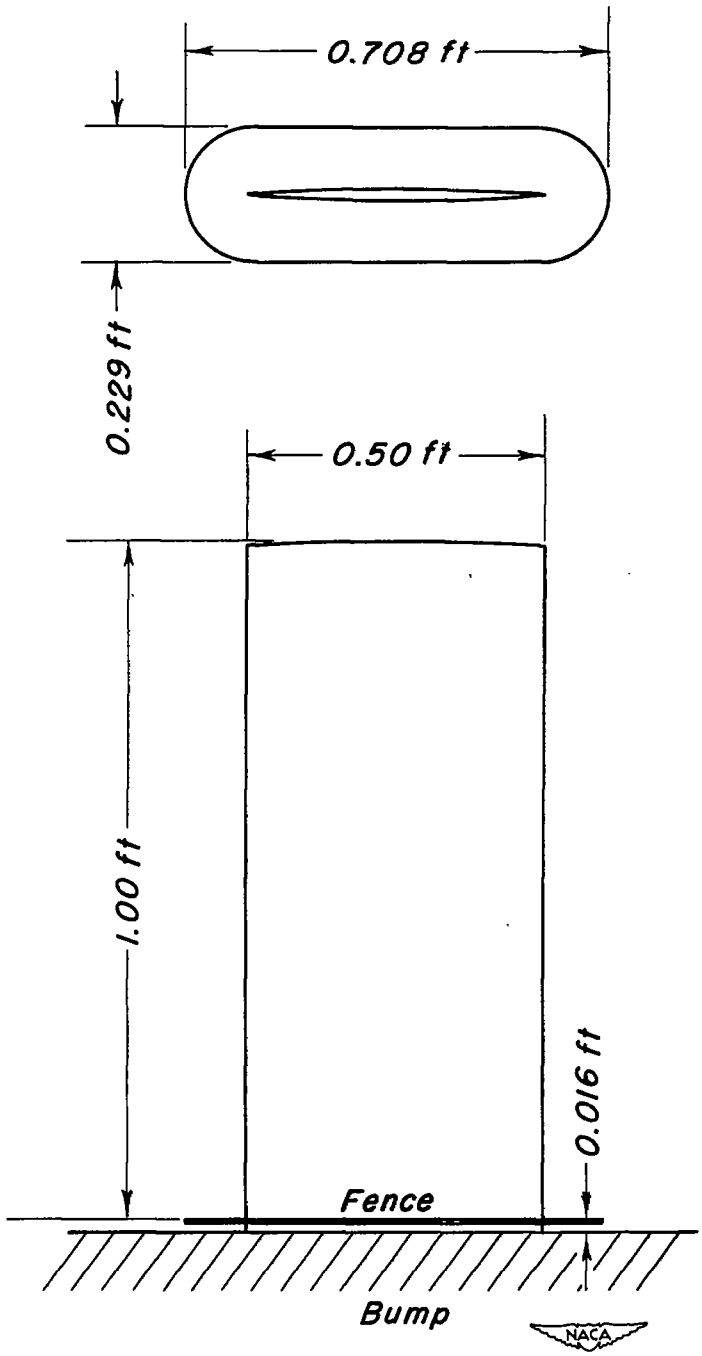

Figure 2.-Dimensions of the rectangular wings.

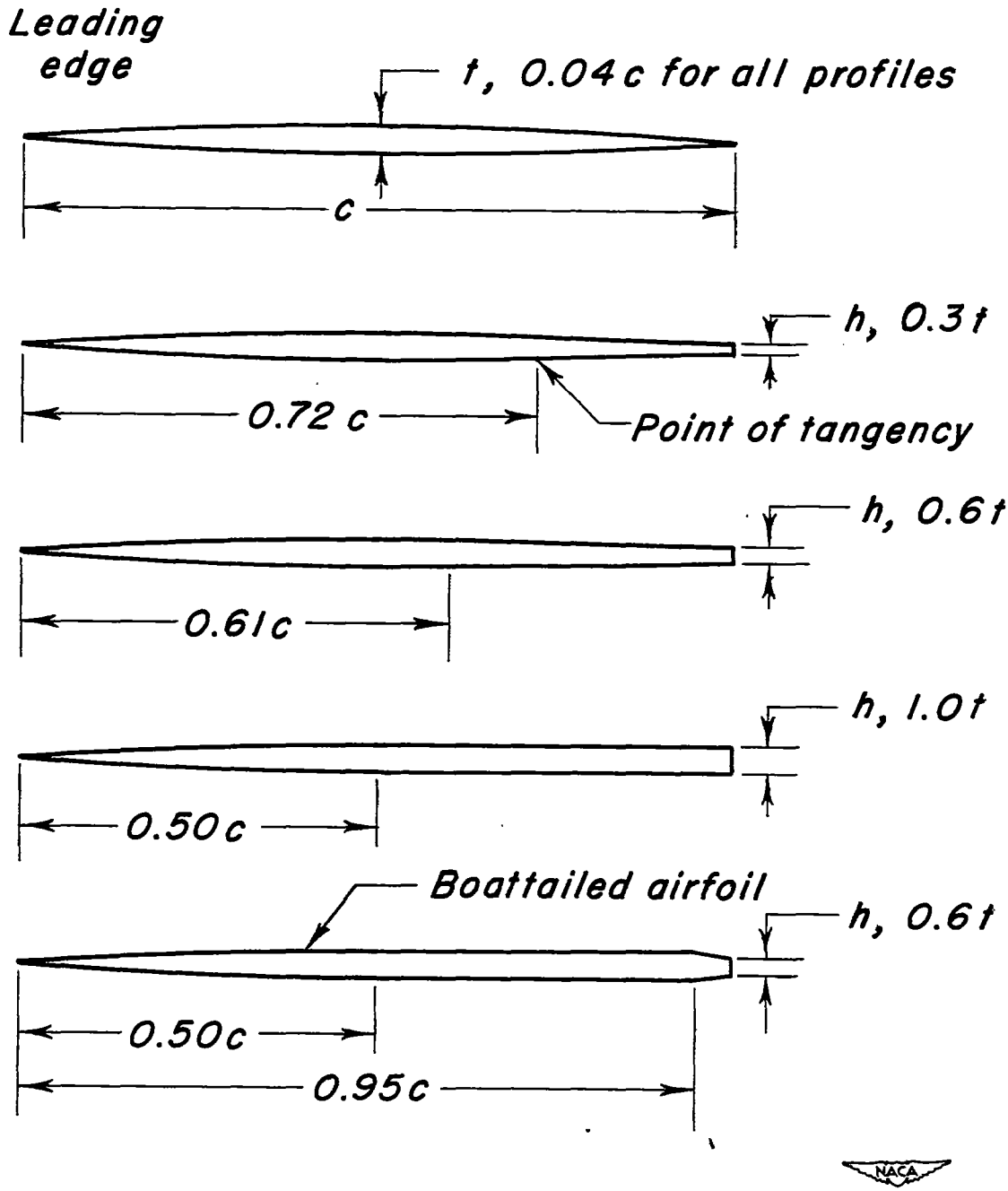

Figure 3.— Airfoil profiles.

CONFIDENTIAL

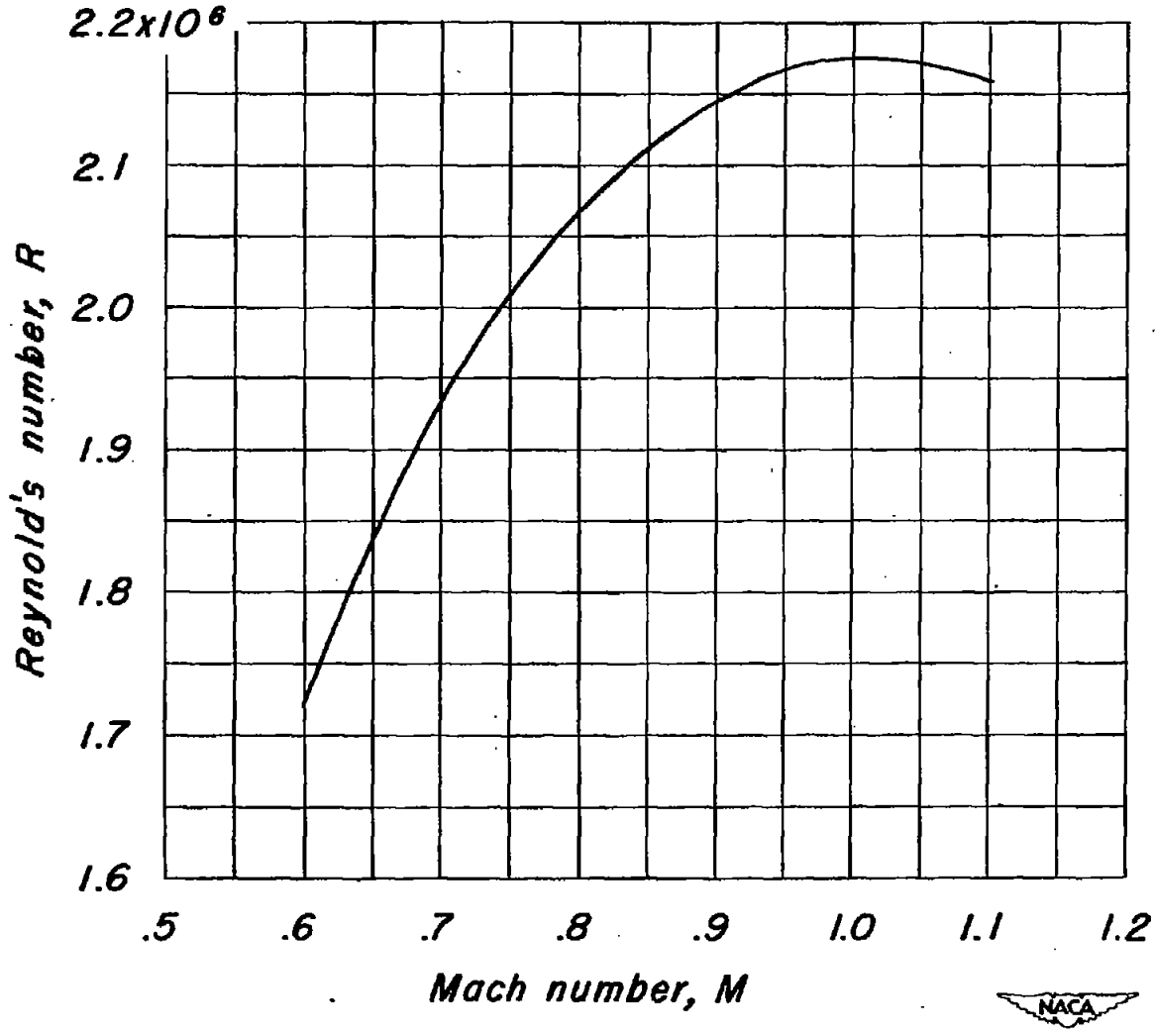

Figure 4.–Variation of Reynold's number with Mach number.

CONFIDENTIAL

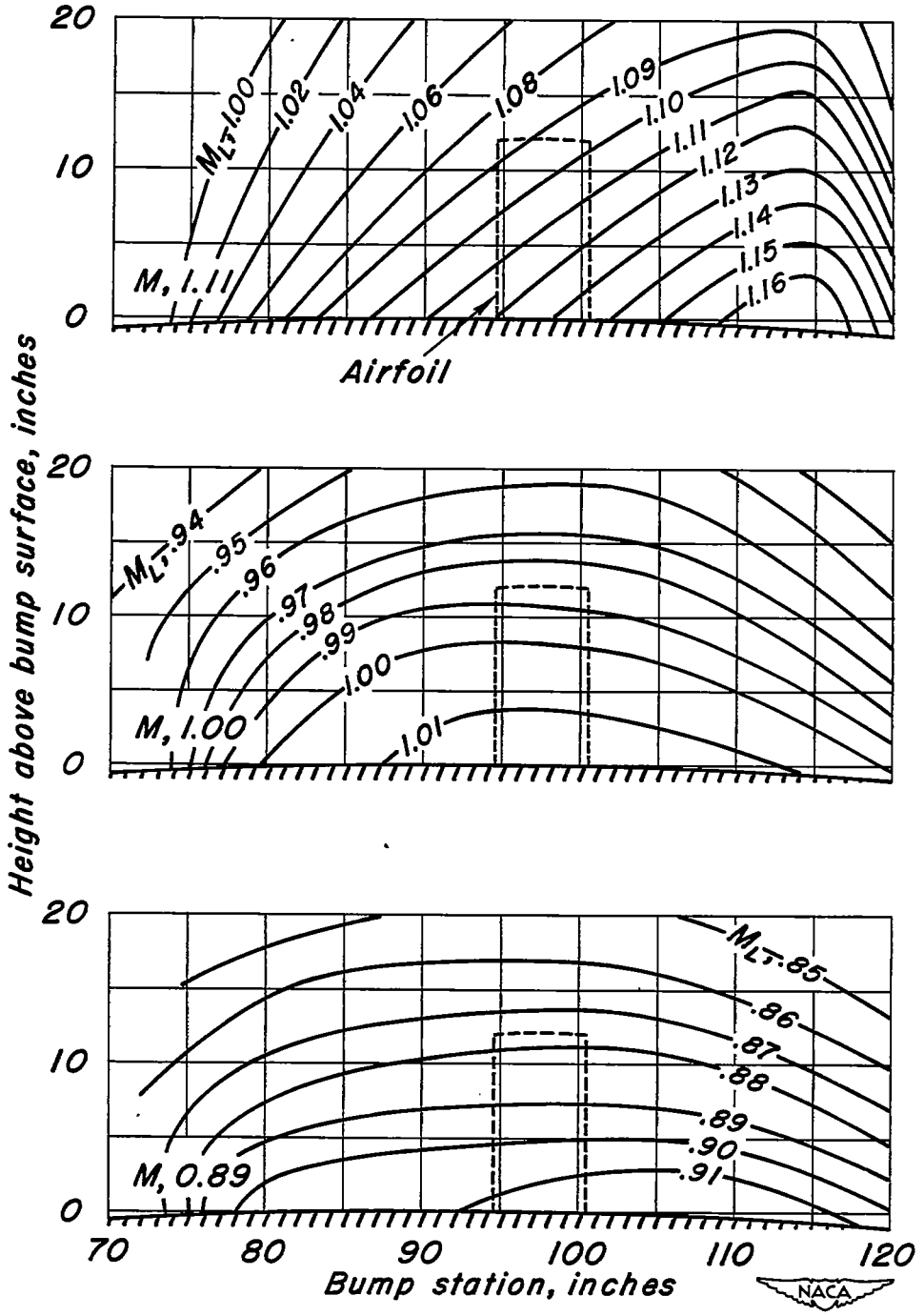

Figure 5.- Typical Mach number contours of the Ames 16-foot wind-tunnel transonic bump.

CONFIDENTIAL

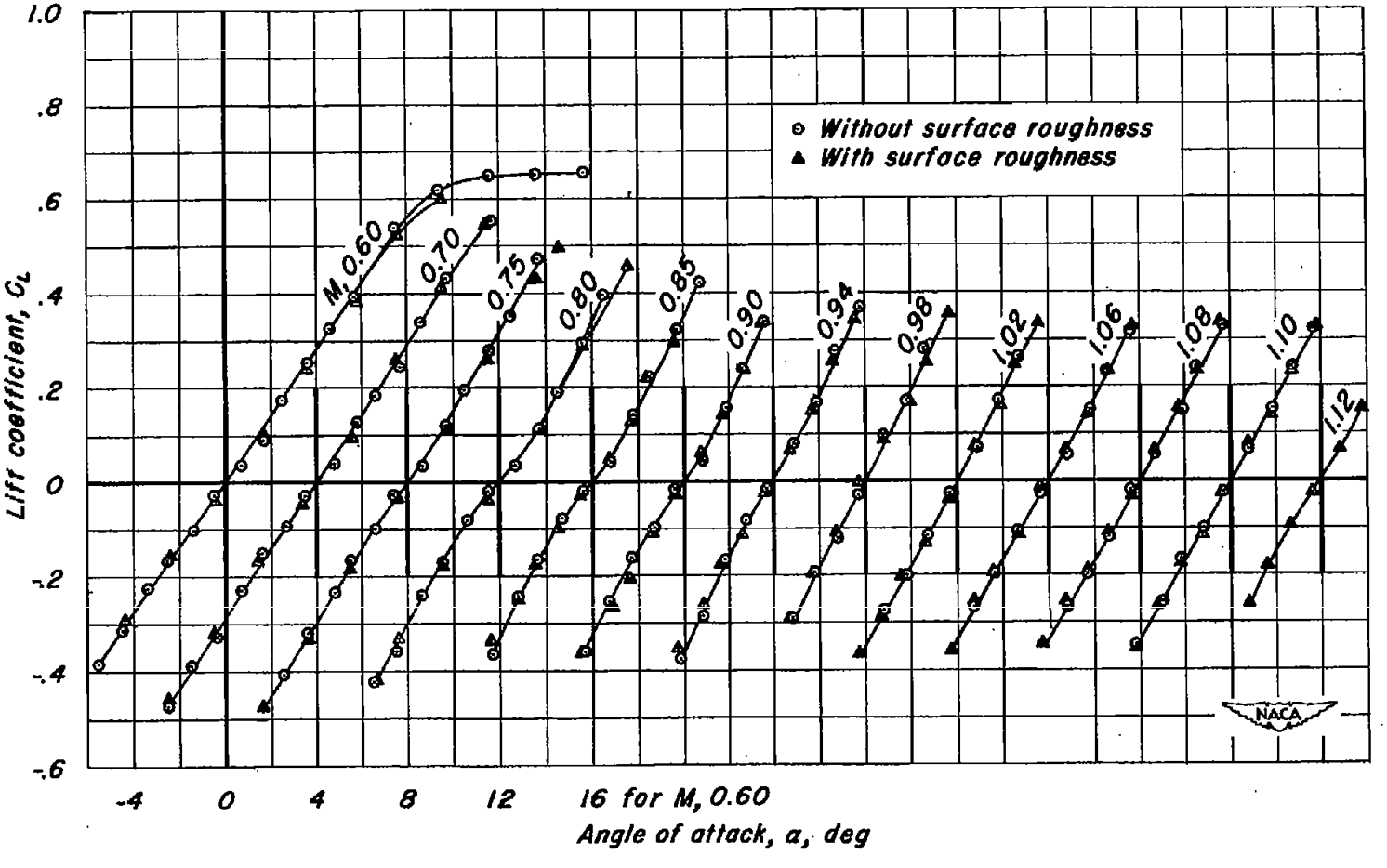

(a) C_L vs α.

Figure 6.—Aerodynamic characteristics at various Mach numbers. Circular-arc profile, $\frac{t}{l}$, 0.

CONFIDENTIAL

CONFIDENTIAL

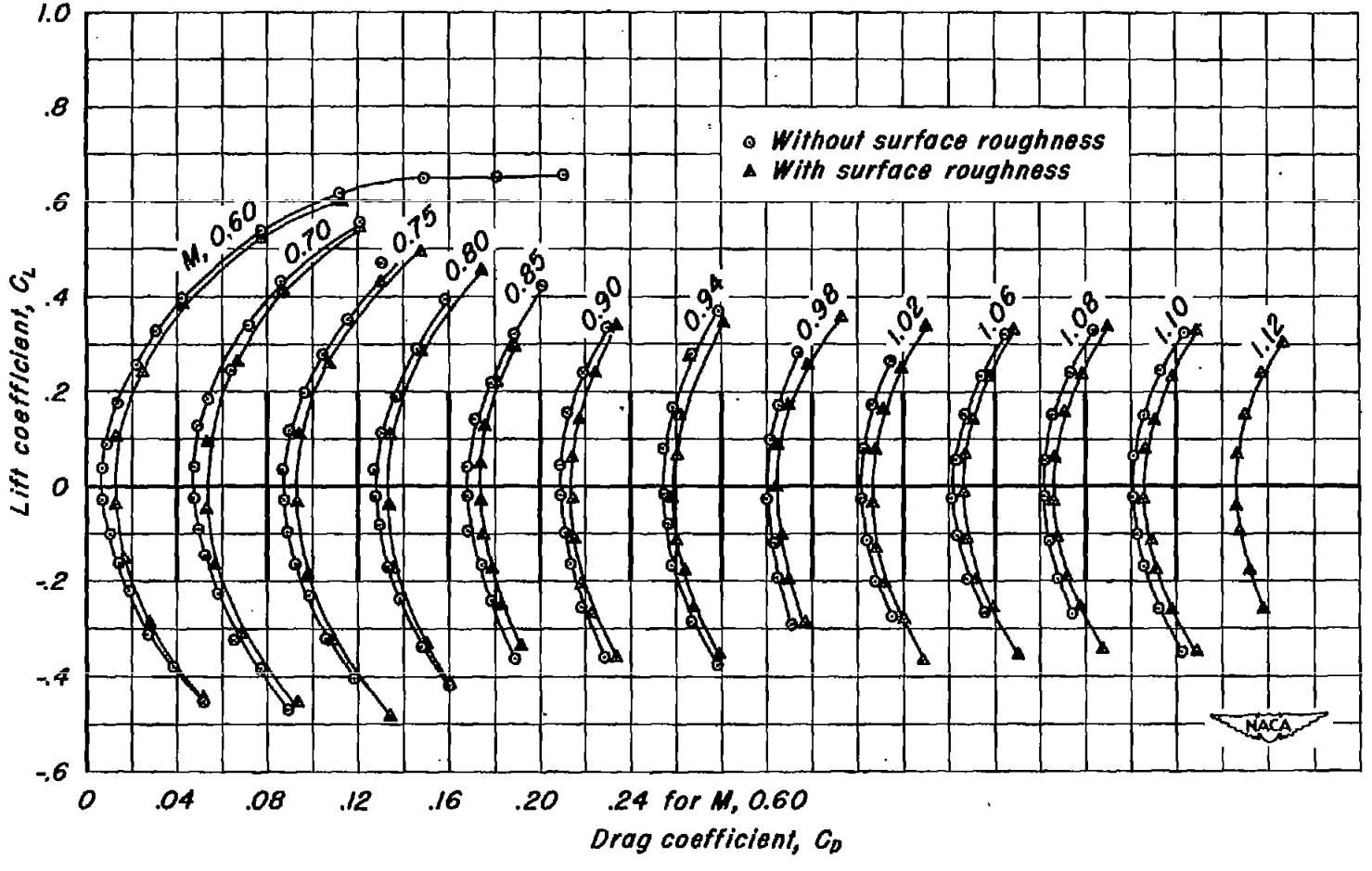

(b) C_L vs C_D

Figure 6.— Continued.

CONFIDENTIAL

CONFIDENTIAL

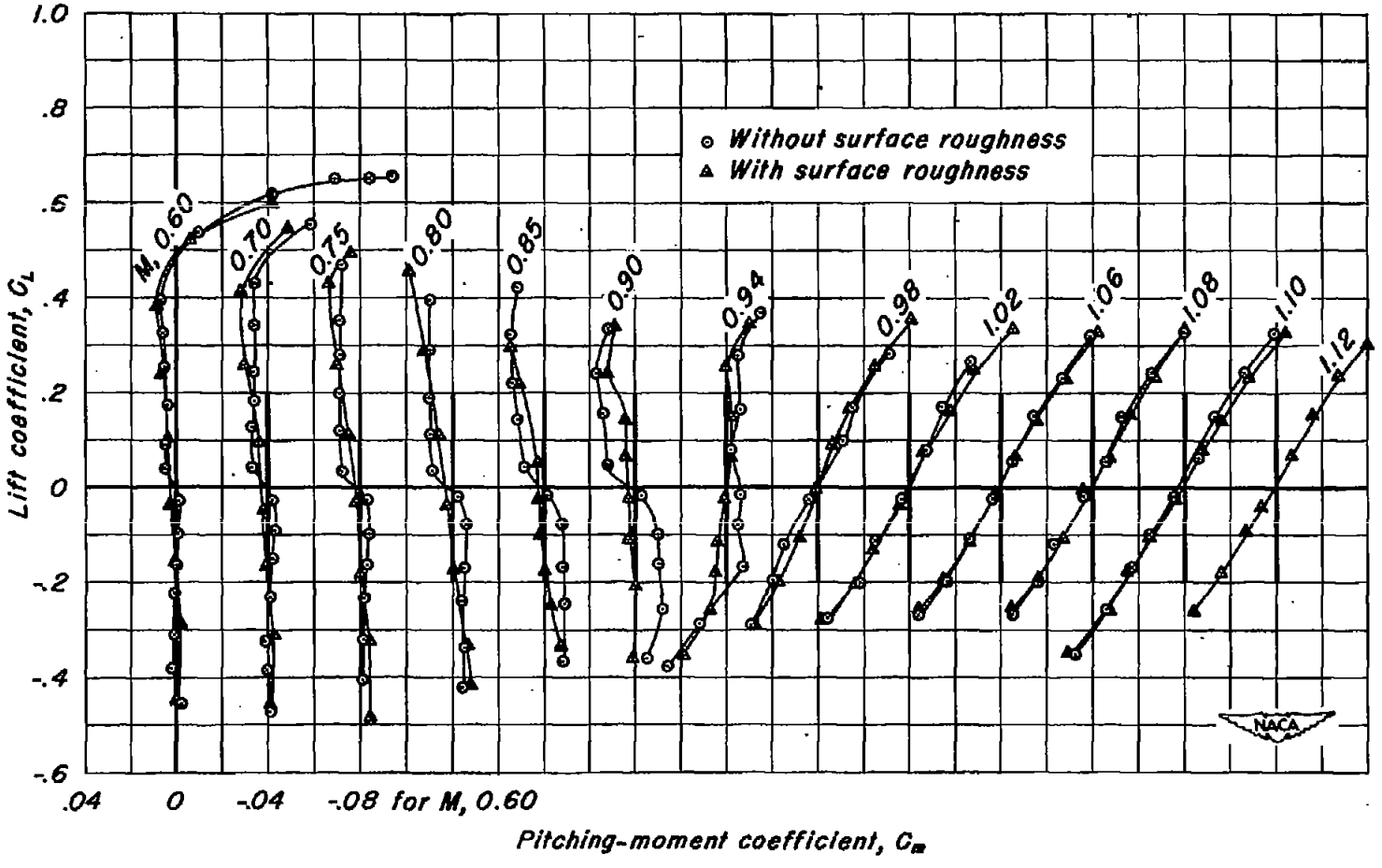

(c) C_L vs C_m

Figure 6.—Concluded.

CONFIDENTIAL

CONFIDENTIAL

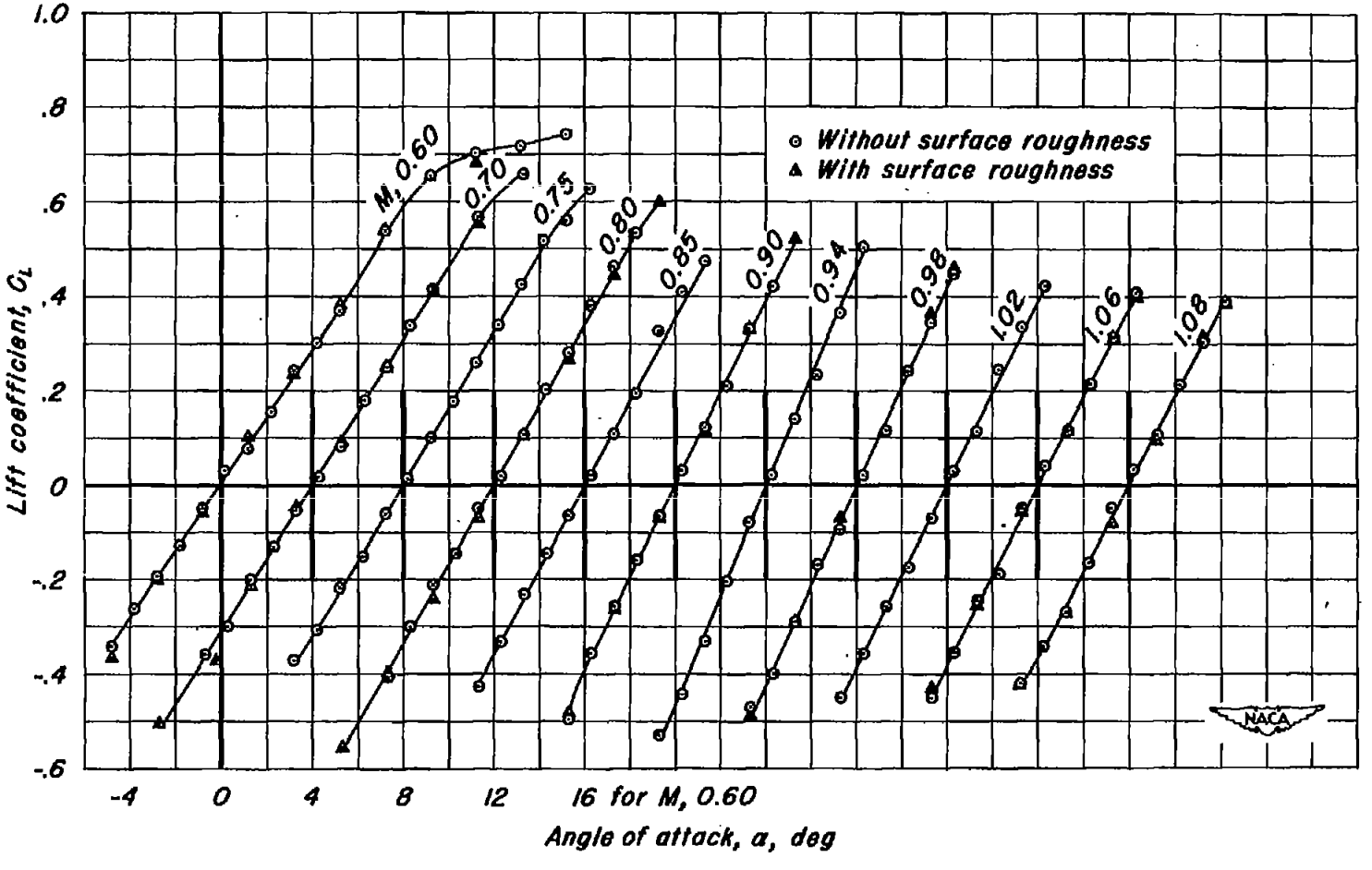

(a) C_L vs α

Figure 7.—Aerodynamic characteristics at various Mach numbers. Blunt-trailing-edge profile, $\frac{h}{t}$, 0.30.

CONFIDENTIAL

CONFIDENTIAL

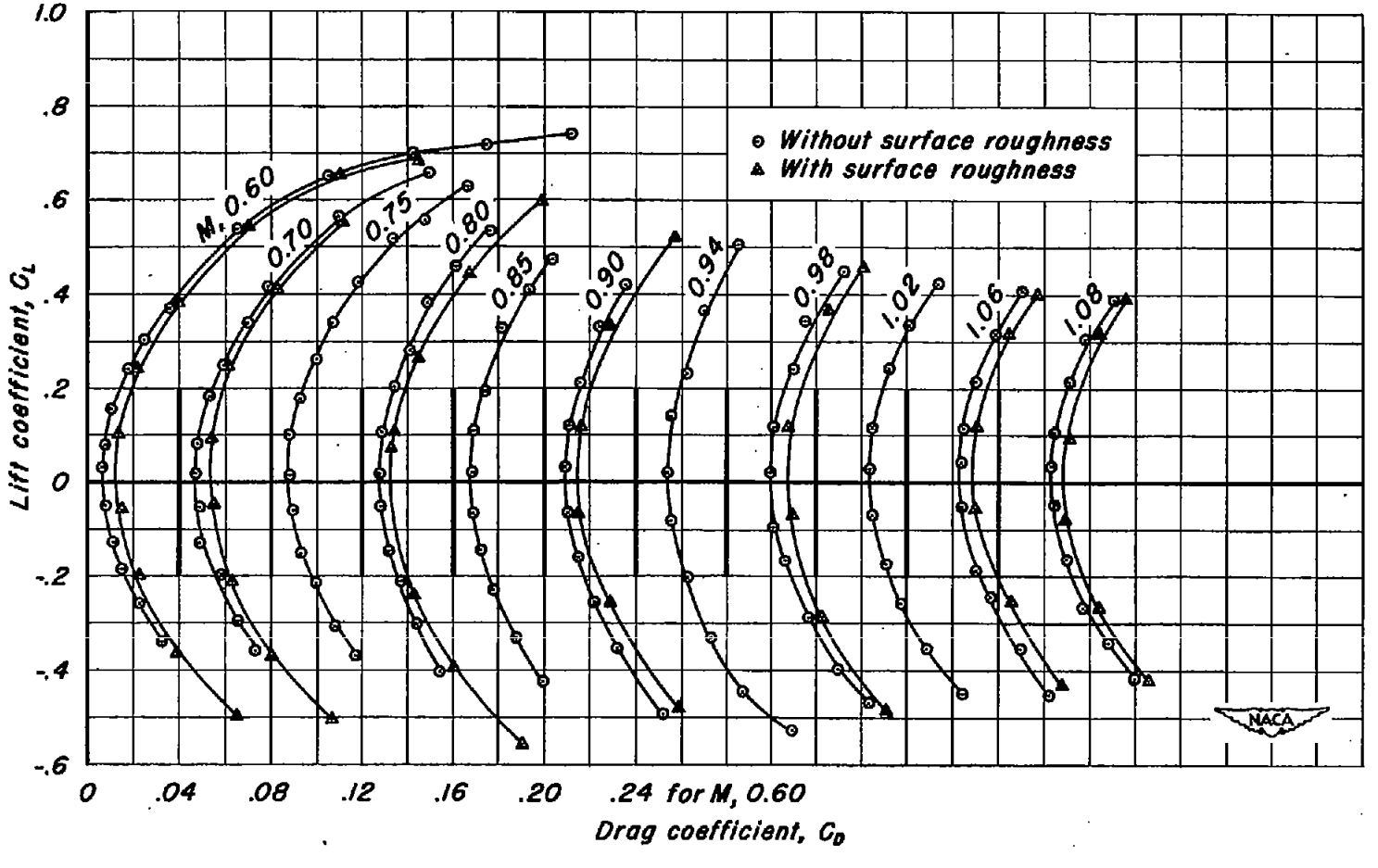

(b) C_L vs C_D

Figure 7.—Continued.

CONFIDENTIAL

CONFIDENTIAL

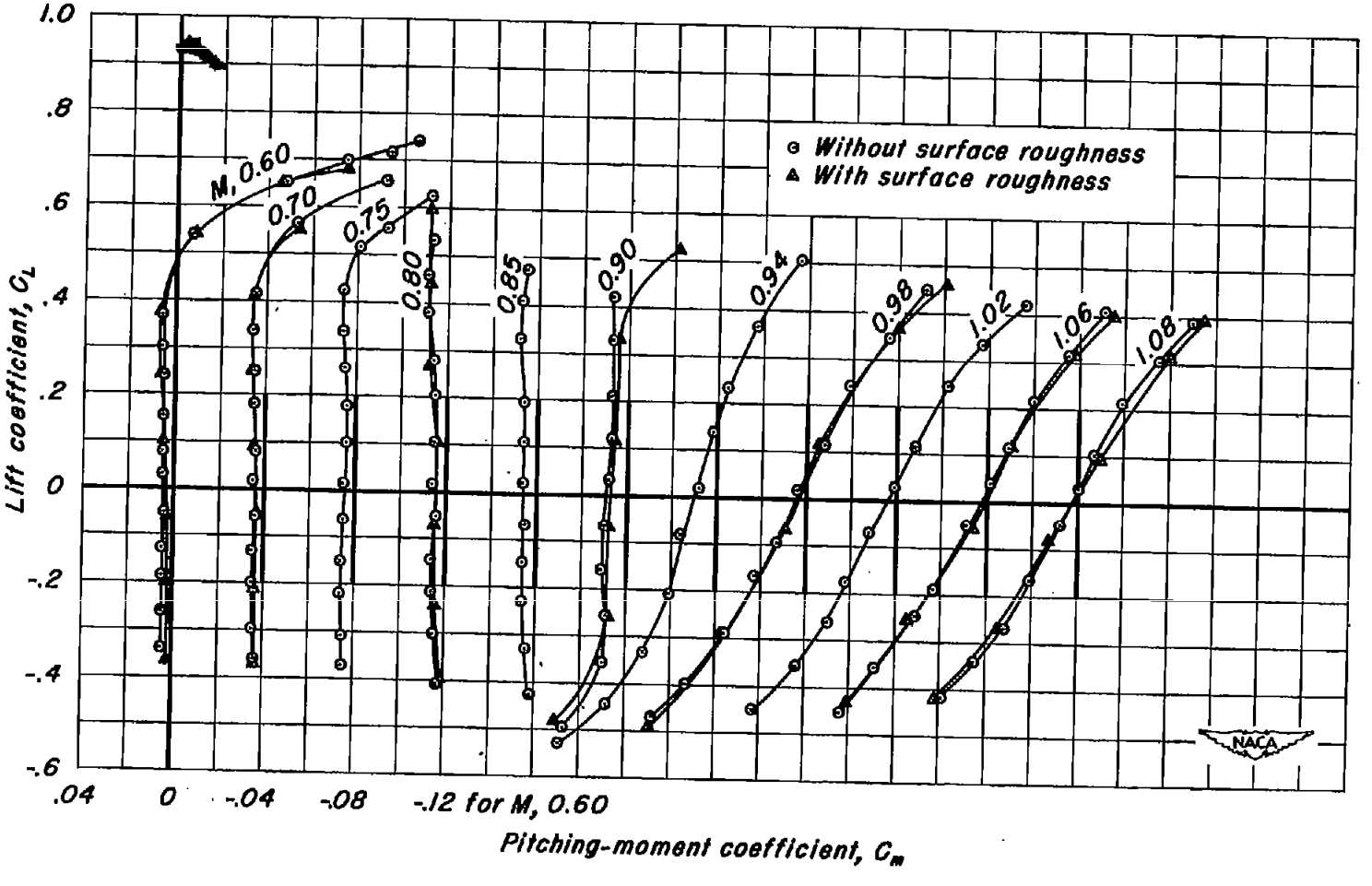

(c) C_L vs C_m

Figure 7.—Concluded.

CONFIDENTIAL

CONFIDENTIAL

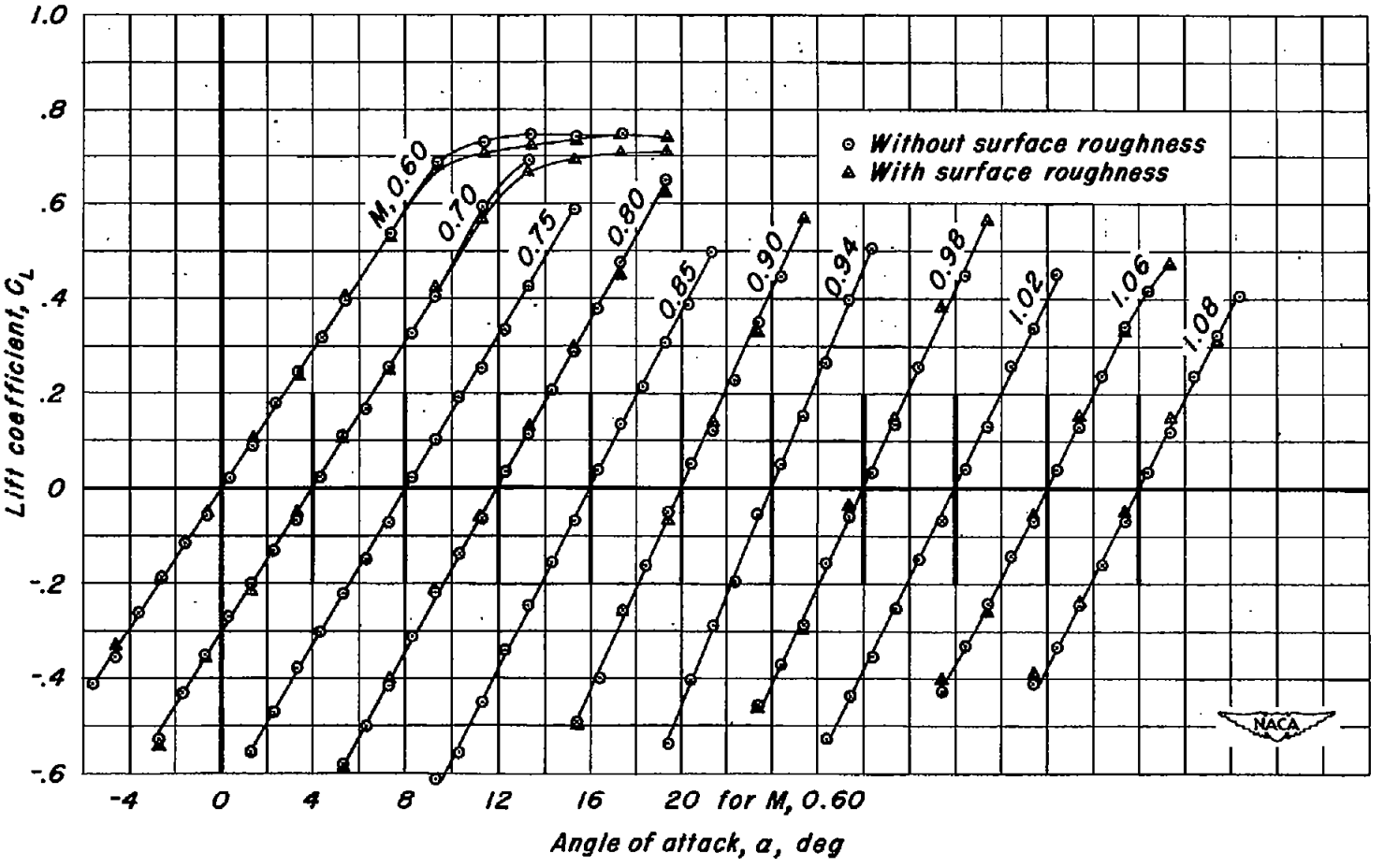

(a) C_L vs α

Figure 8.– Aerodynamic characteristics at various Mach numbers. Blunt-trailing-edge profile, $\frac{t}{l}$, 0.60.

CONFIDENTIAL

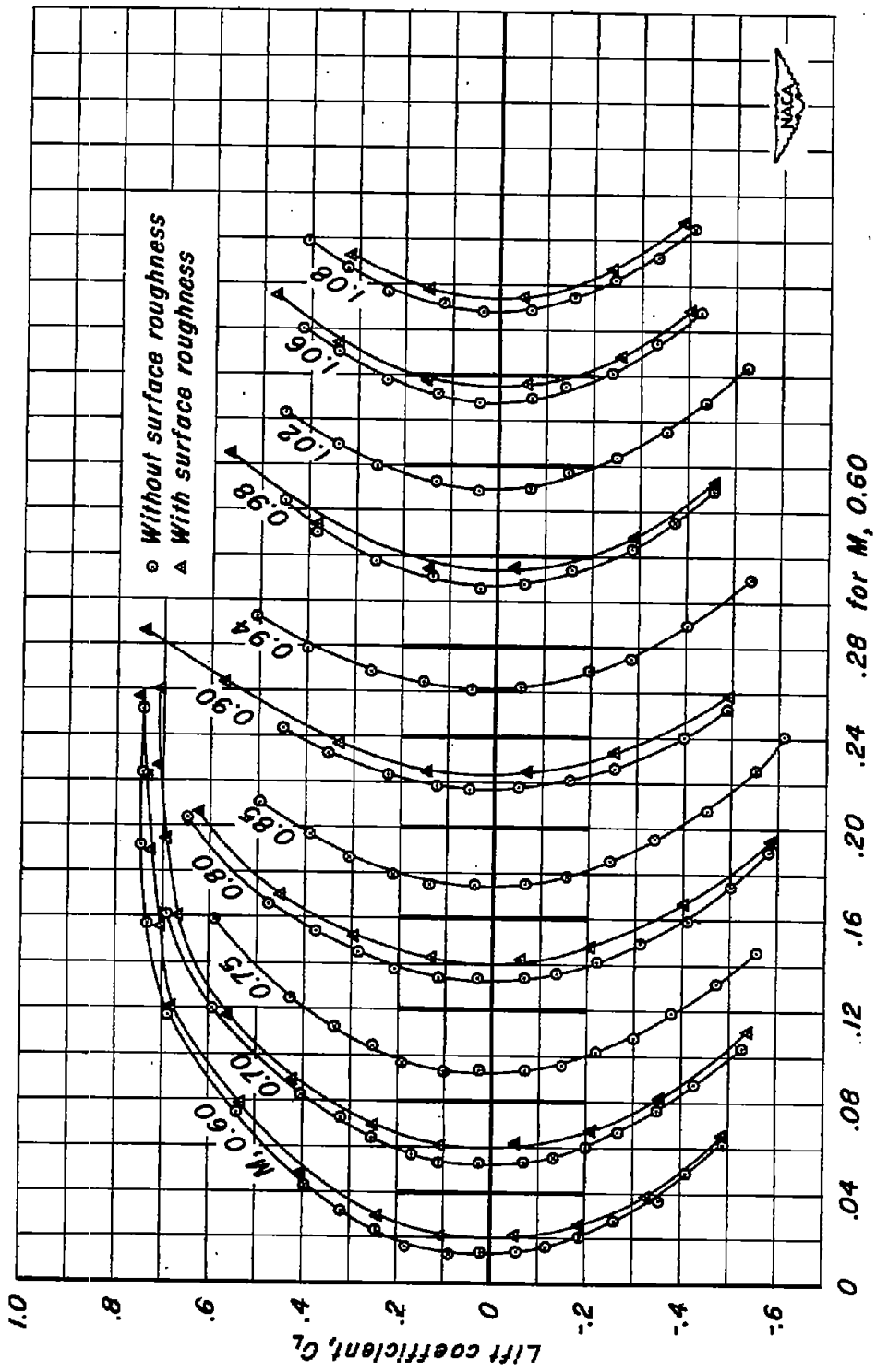

(b) C_L vs C_D

Figure 8.- Continued.

CONFIDENTIAL

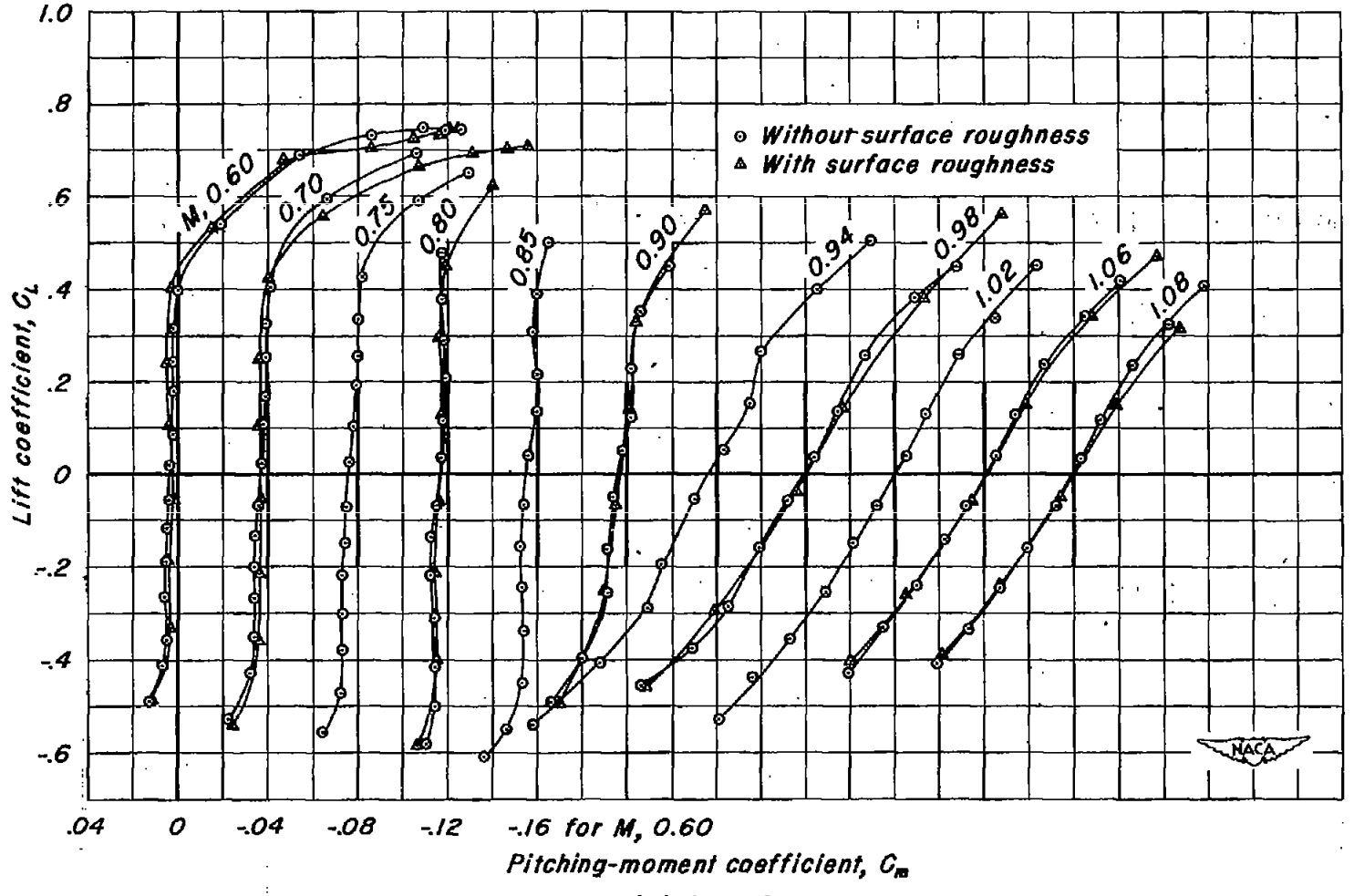

(c) C_L vs C_m

Figure 8.—Concluded.

CONFIDENTIAL

CONFIDENTIAL

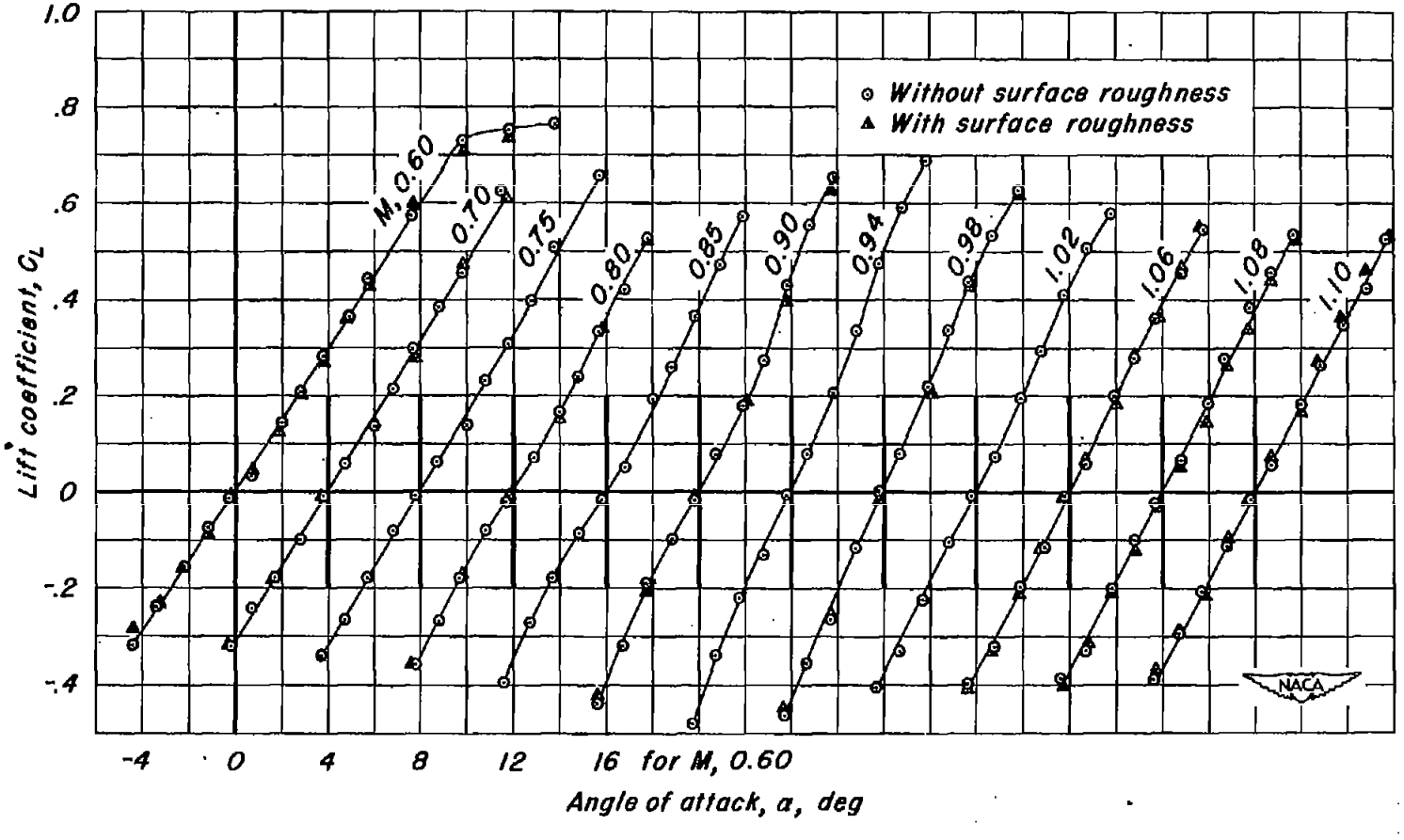

(a) C_L vs α

Figure 9.—Aerodynamic characteristics at various Mach numbers. Blunt-trailing-edge profile, $\frac{h}{t}$, 1.00.

CONFIDENTIAL

CONFIDENTIAL

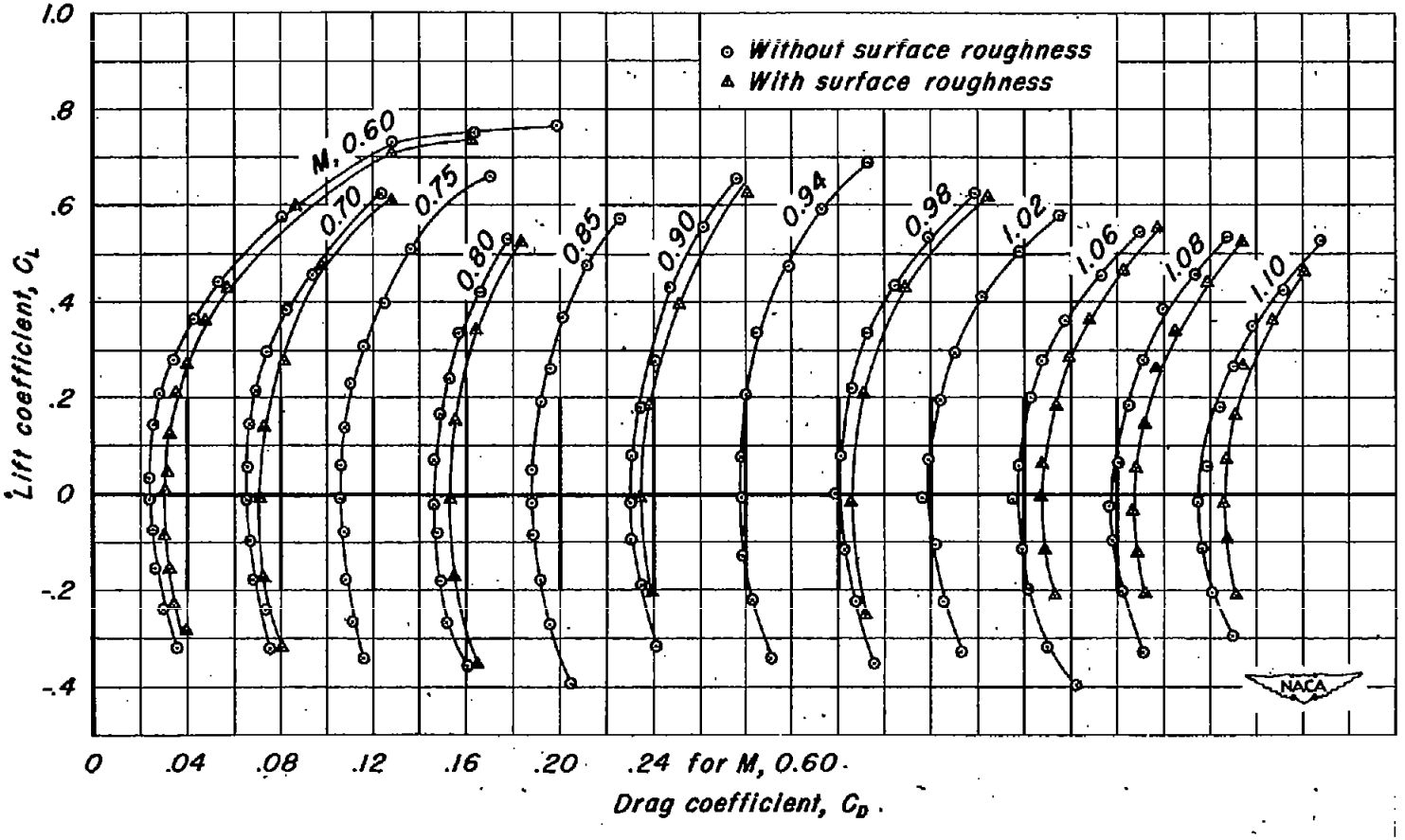

(b) C_L vs C_D

Figure 9.–Continued.

CONFIDENTIAL

CONFIDENTIAL

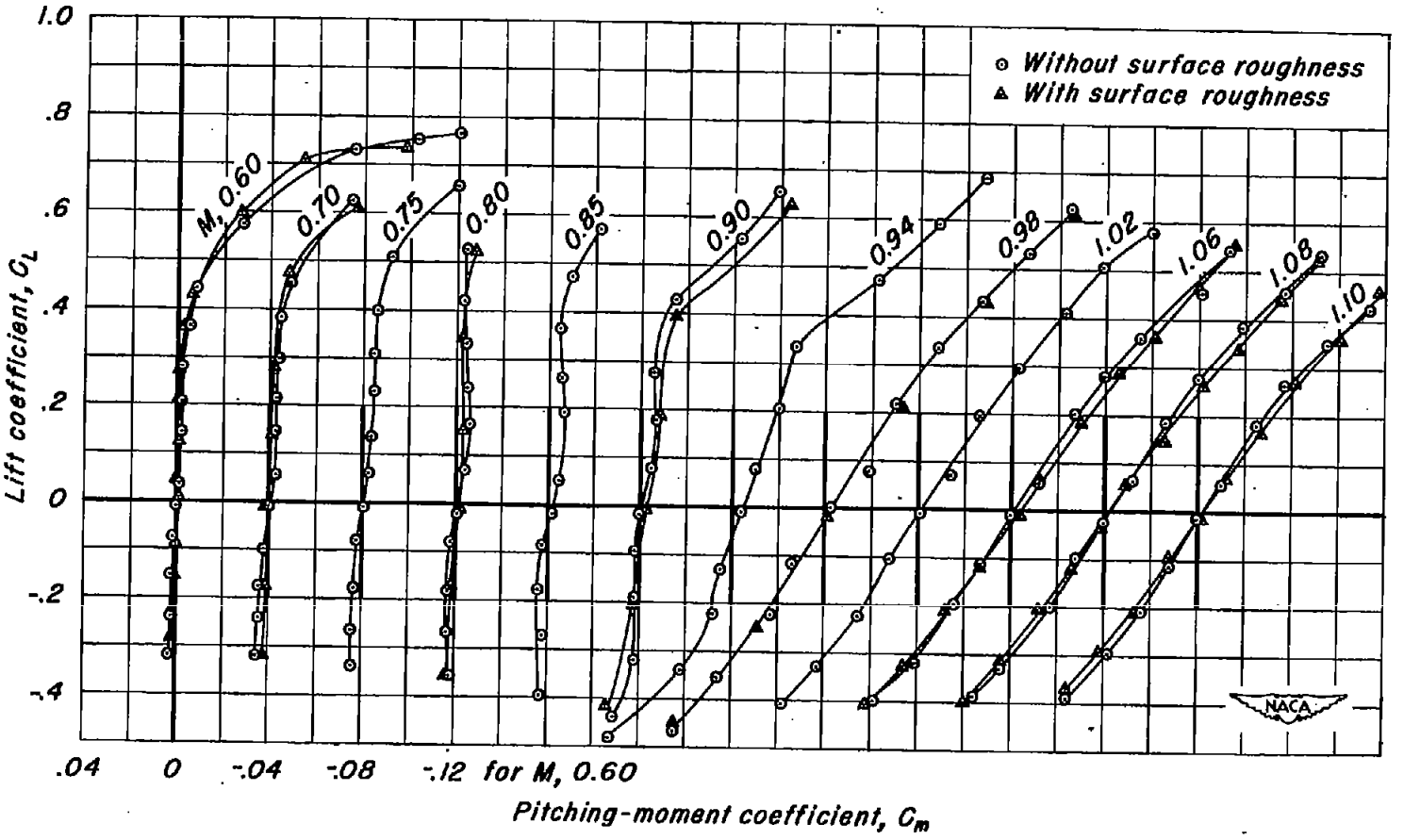

(c) C_L vs C_m

Figure 9.–Concluded.

CONFIDENTIAL

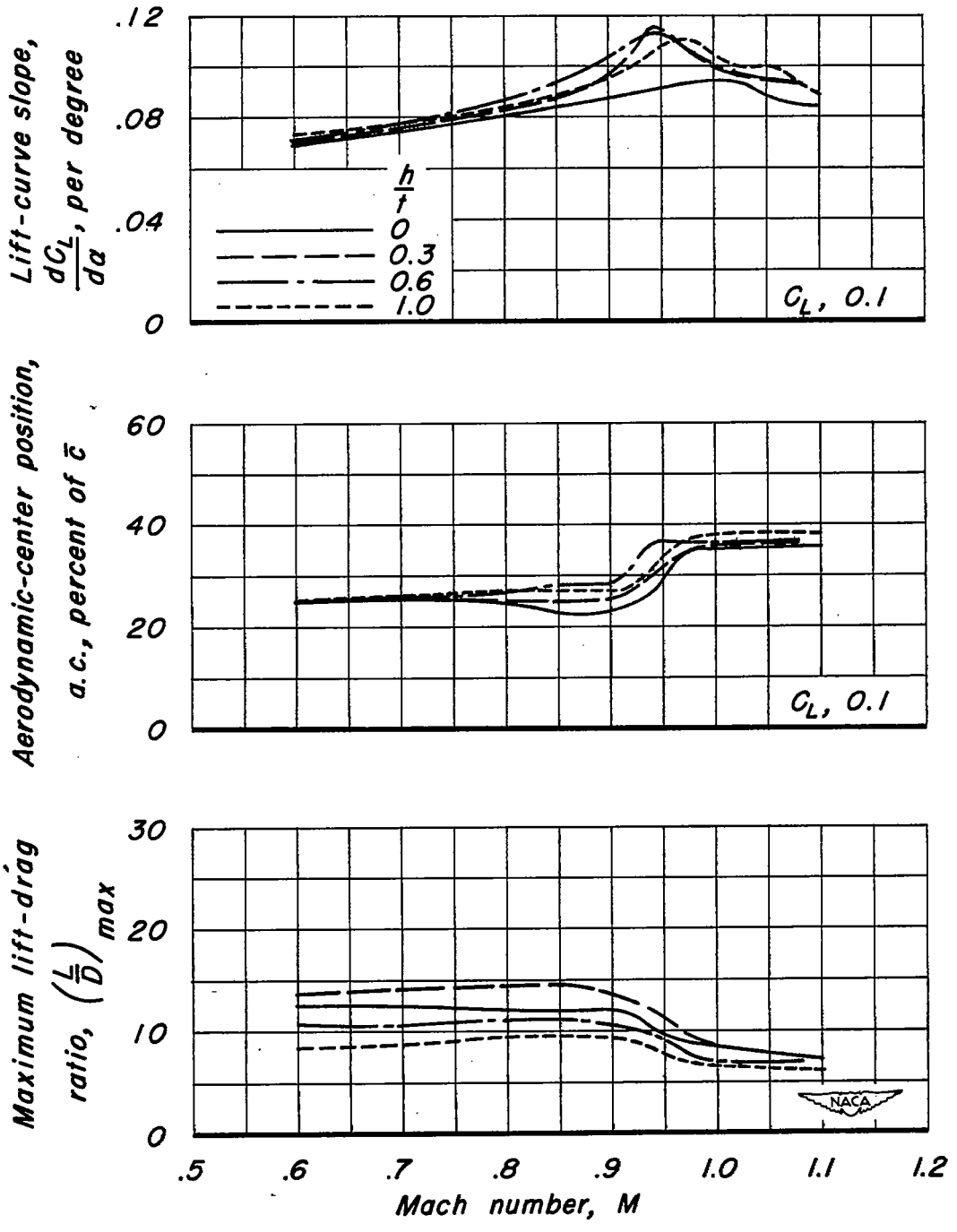

Figure 10.–Variation of aerodynamic parameters with Mach number for blunt-trailing-edge airfoils.

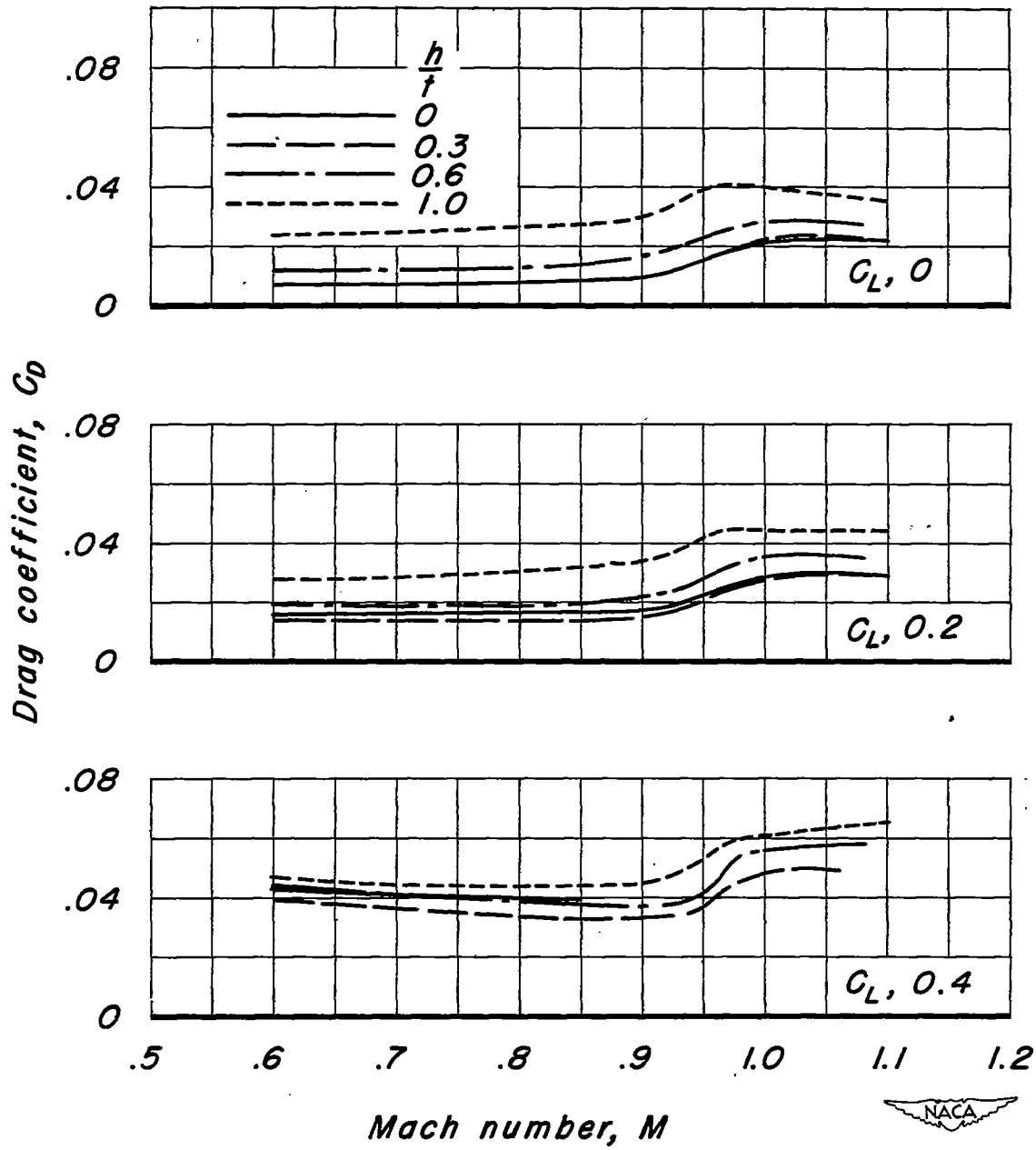

Figure 11.–Drag coefficient as a function of Mach number at various lift coefficients.

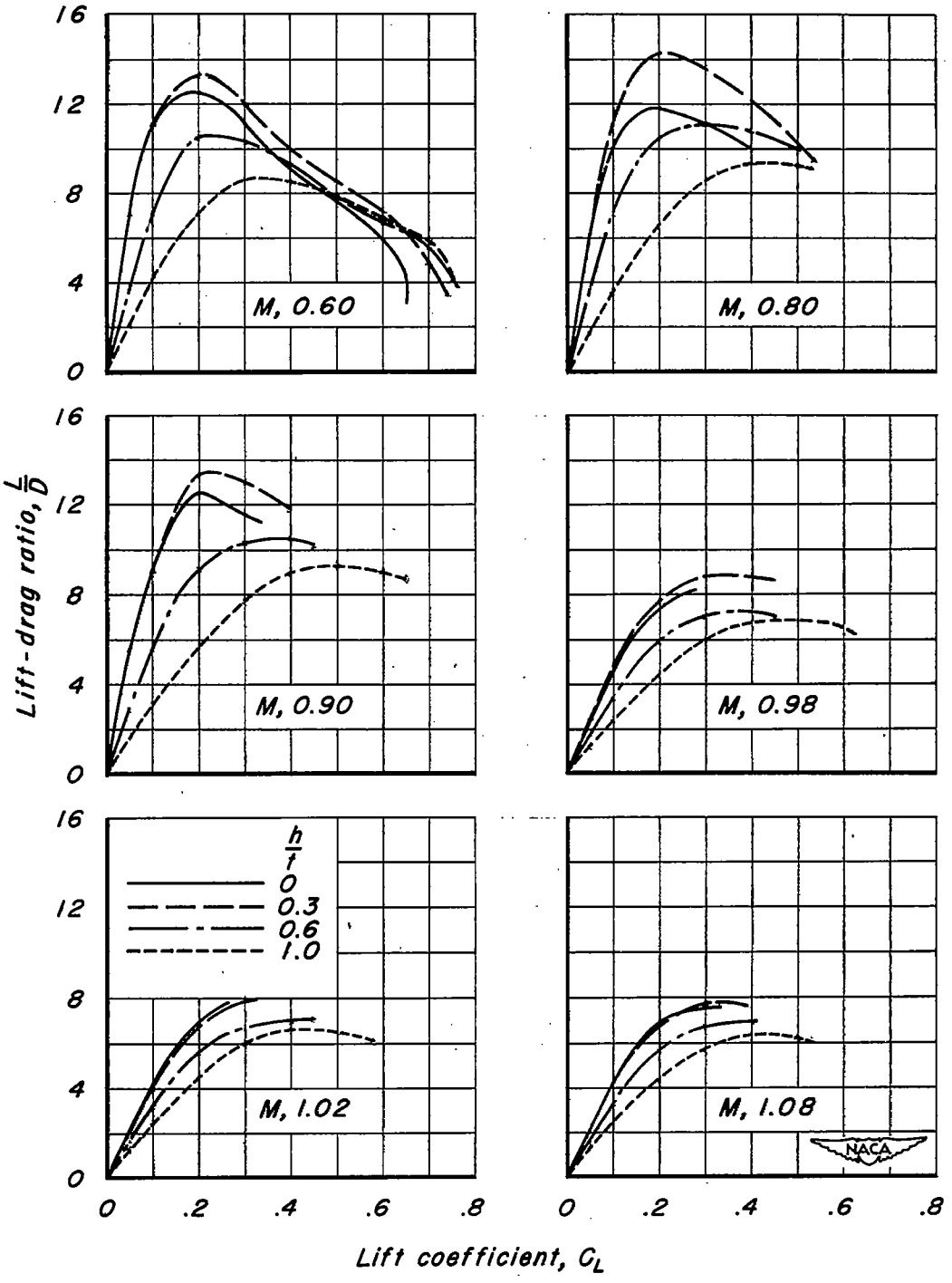

Figure 12.–Lift-drag ratio as a function of lift coefficient at various Mach numbers for different trailing-edge thicknesses.

CONFIDENTIAL

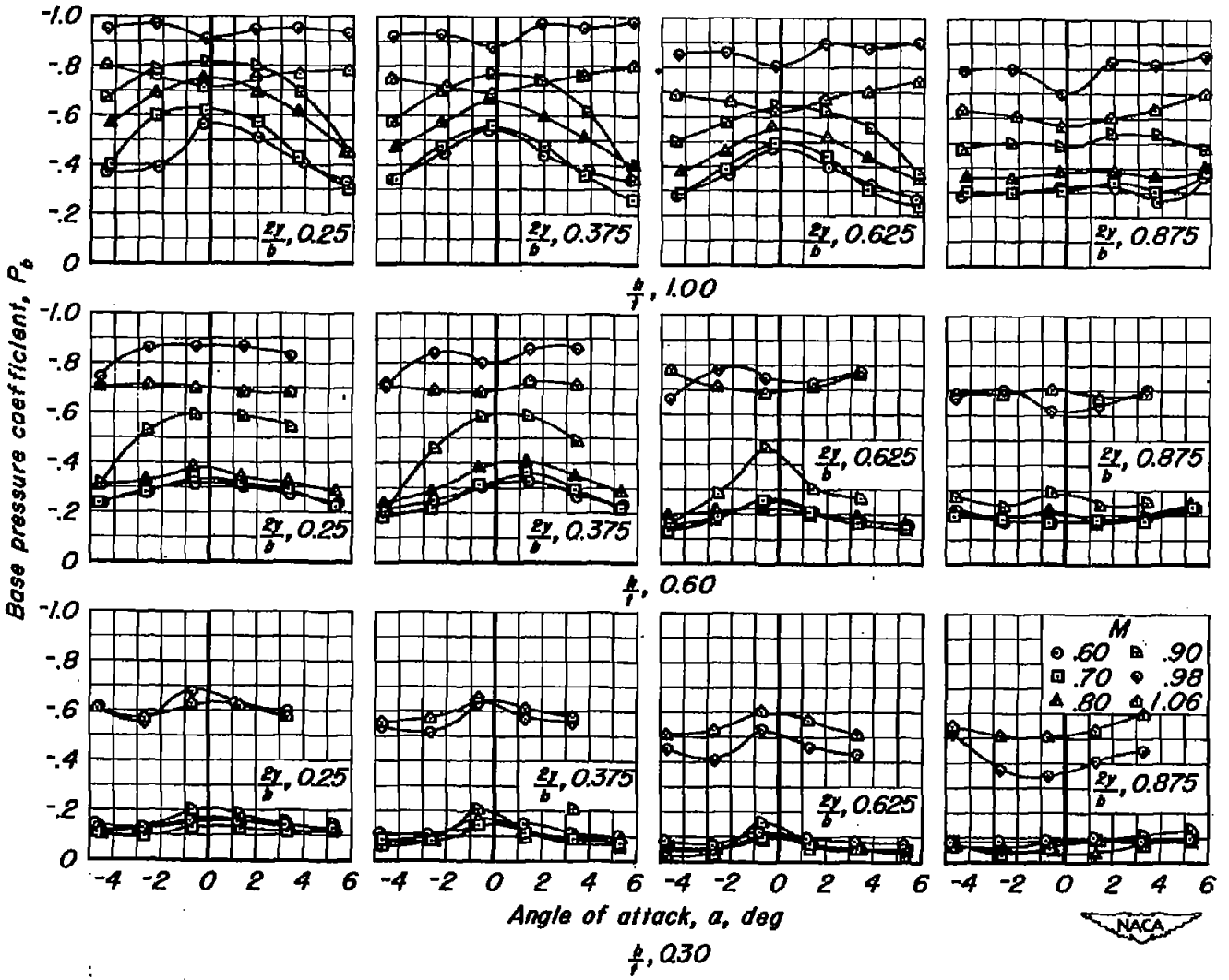

(a) Without surface roughness.

Figure 13.–Base pressure coefficients as a function of angle of attack.

CONFIDENTIAL

CONFIDENTIAL

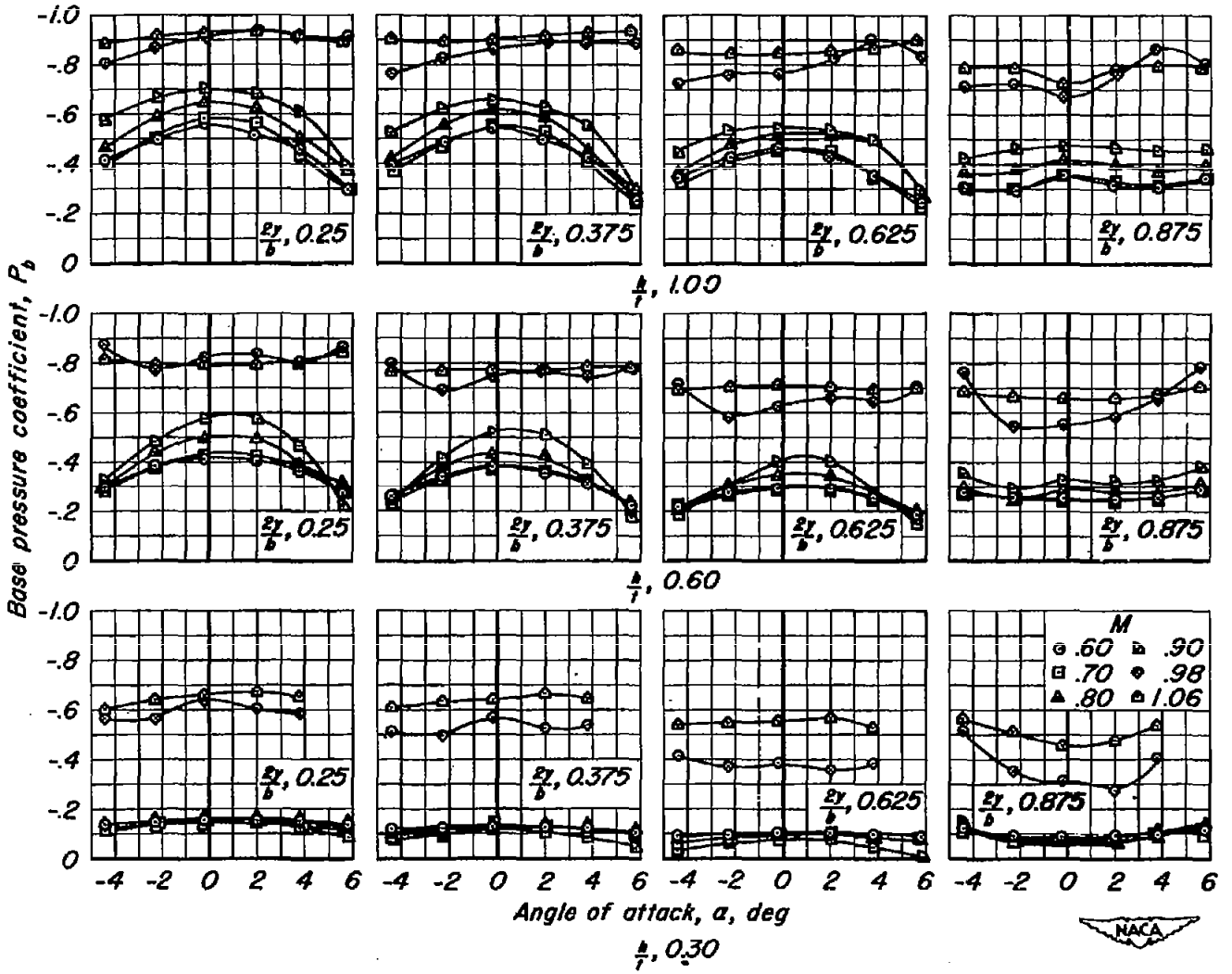

(b) With surface roughness.

Figure 13.–Concluded.

CONFIDENTIAL

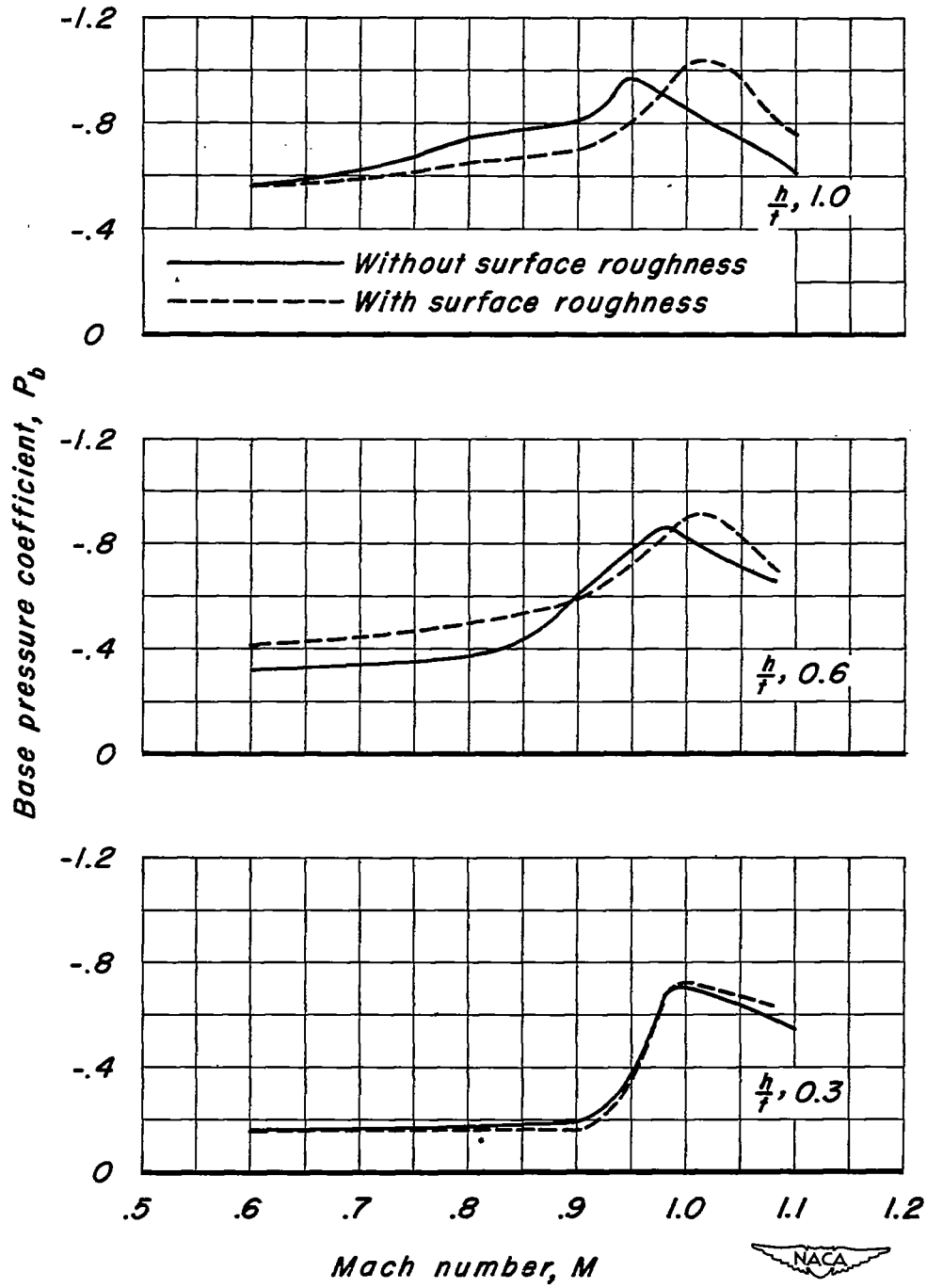

Figure 14.–The variation of base pressure coefficient with Mach number at semispan station $\frac{2y}{b}$ = 0.25. Angle of attack, 0°.

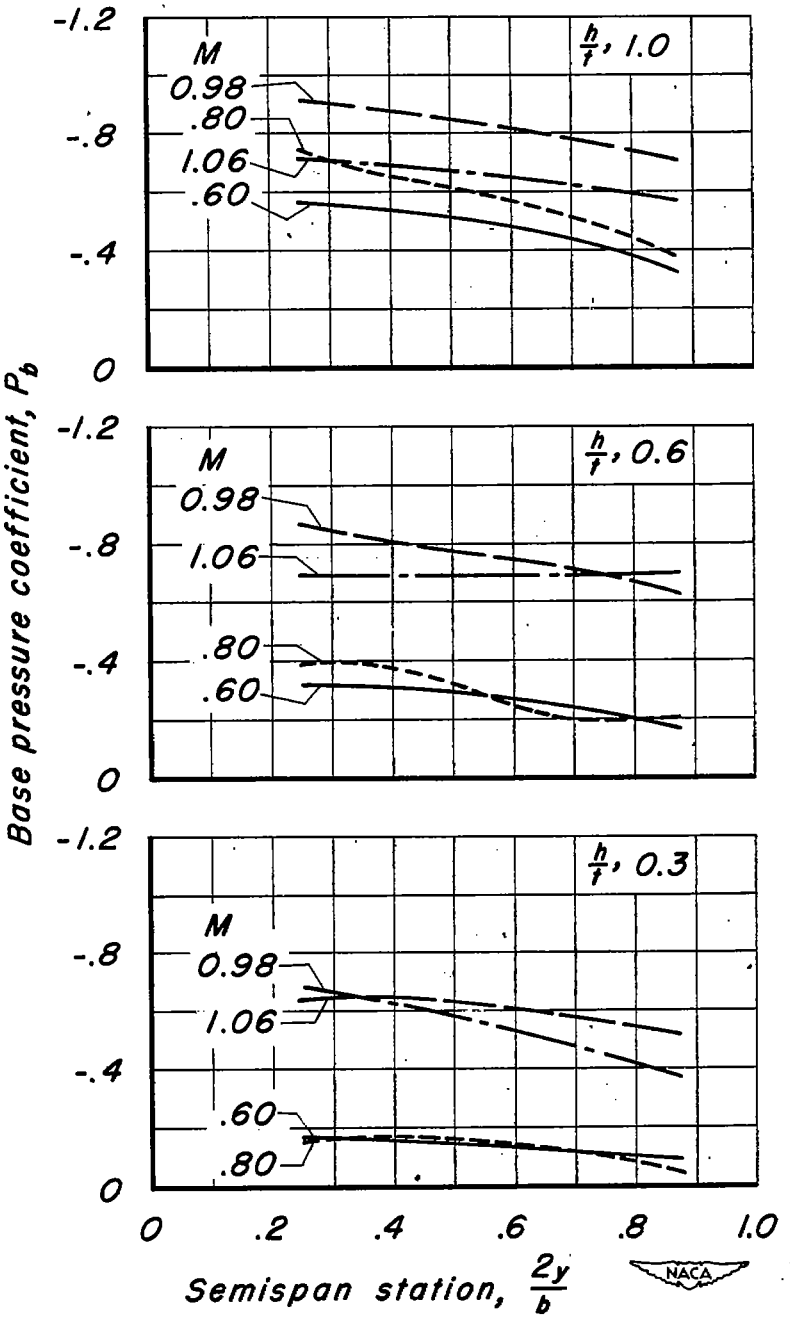

Figure 15.—The variation of base pressure coefficient with semispan station, $\frac{2y}{b}$. Angle of attack, 0°.

CONFIDENTIAL

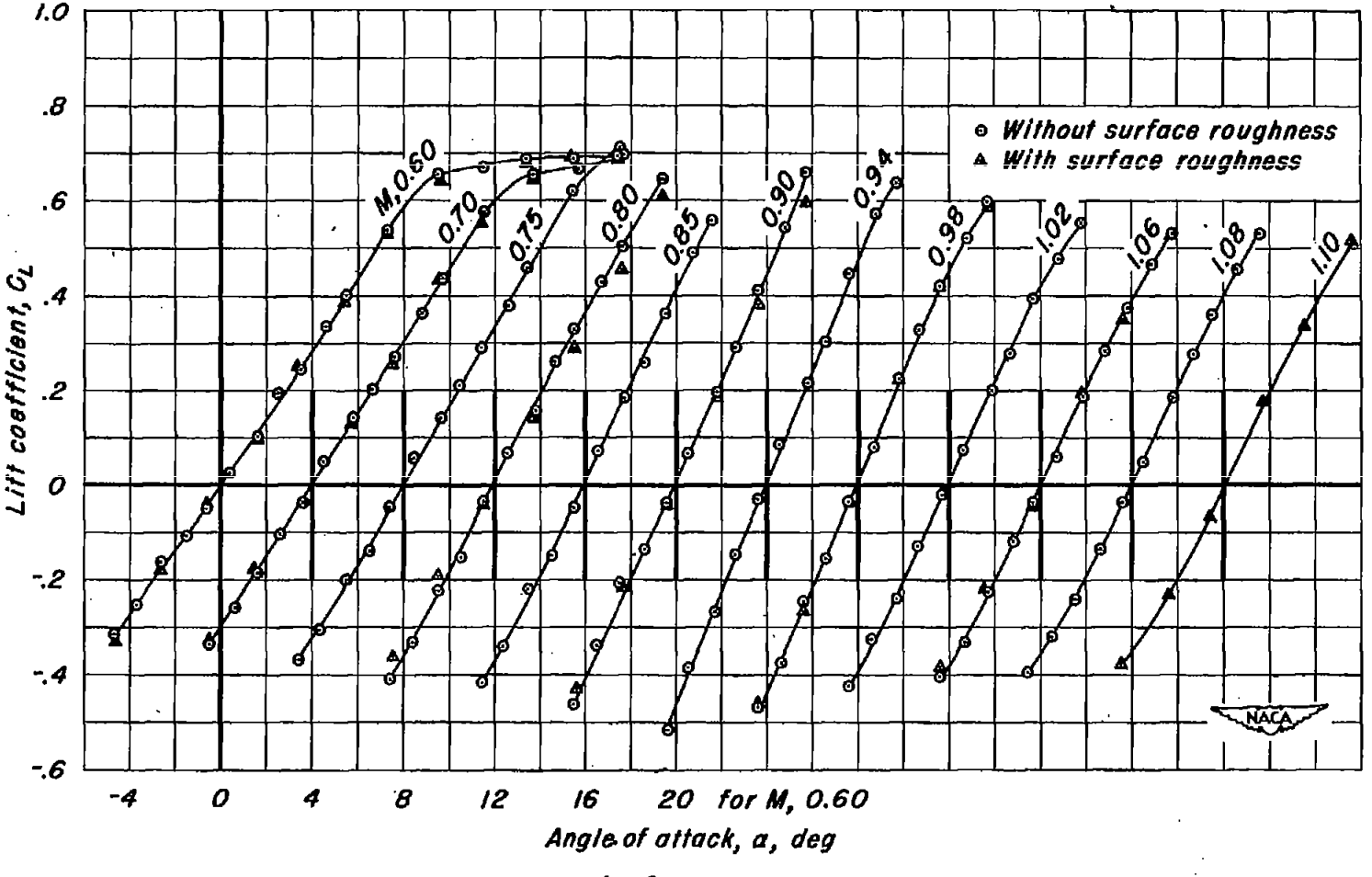

(a) C_L vs α

Figure 16.–Aerodynamic characteristics at various Mach numbers. Boattail trailing edge.

CONFIDENTIAL

CONFIDENTIAL

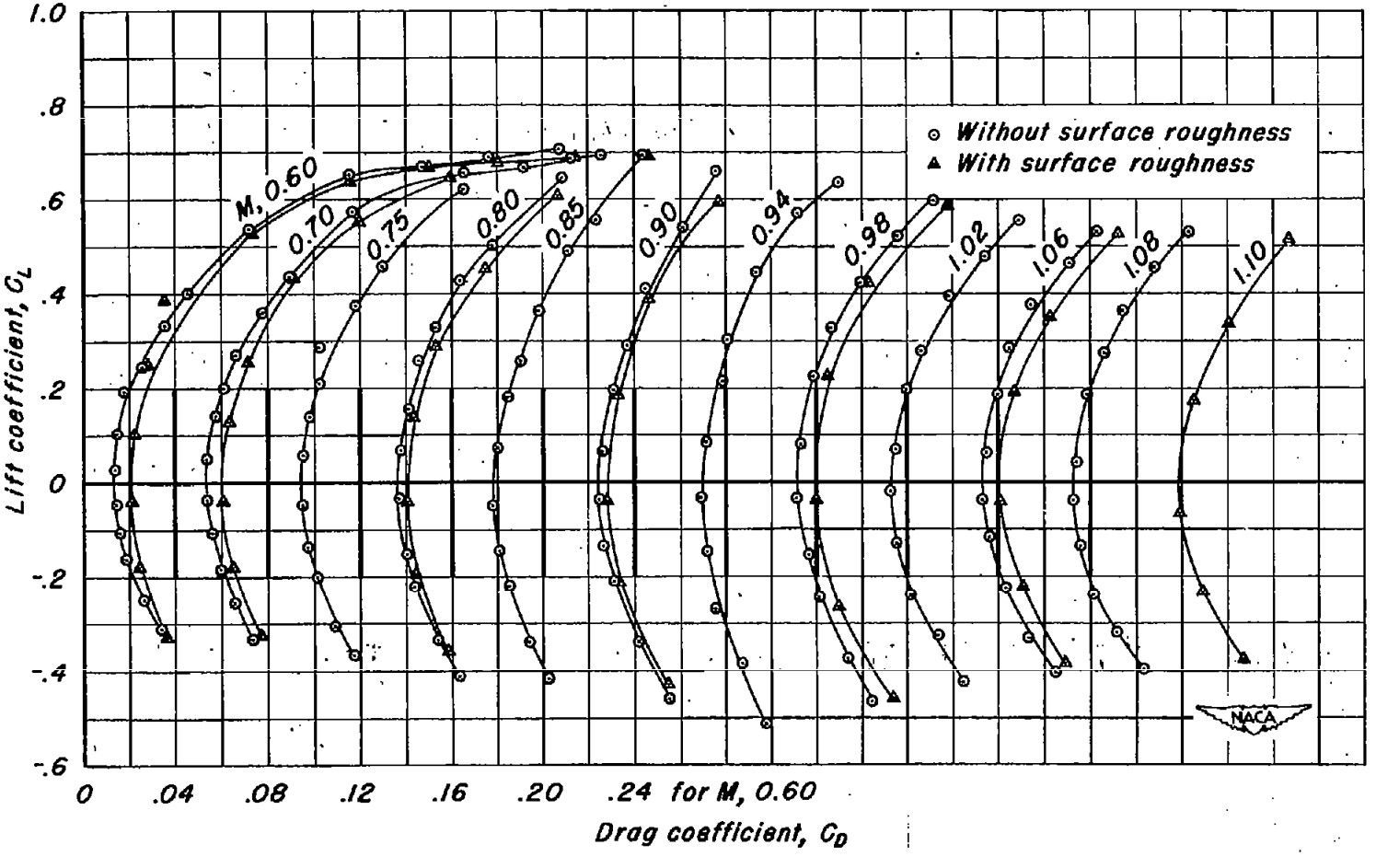

(b) C_L vs C_D

Figure 16.—Continued.

CONFIDENTIAL

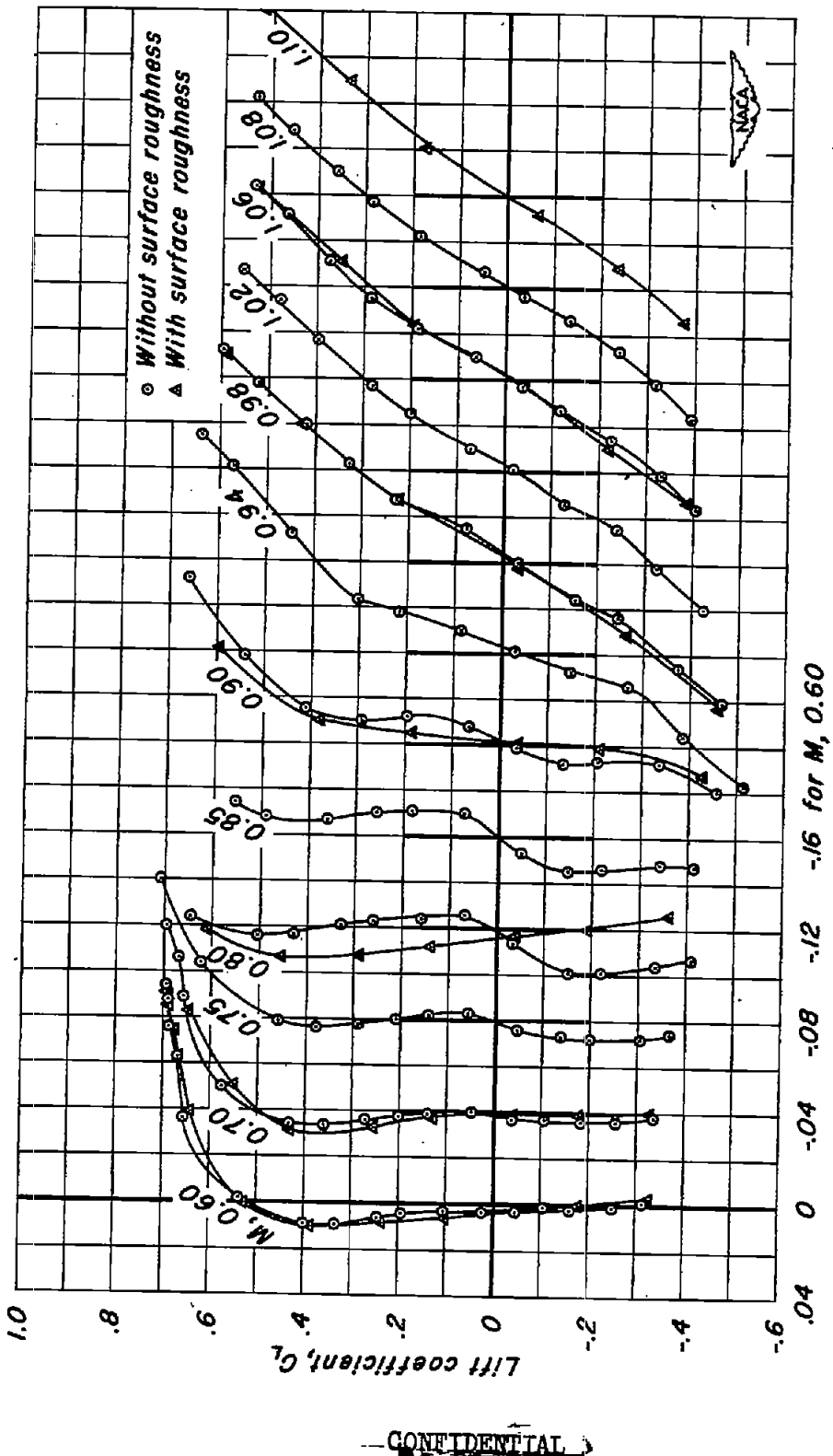

(c) C_L vs C_m

Figure 16.—Concluded.

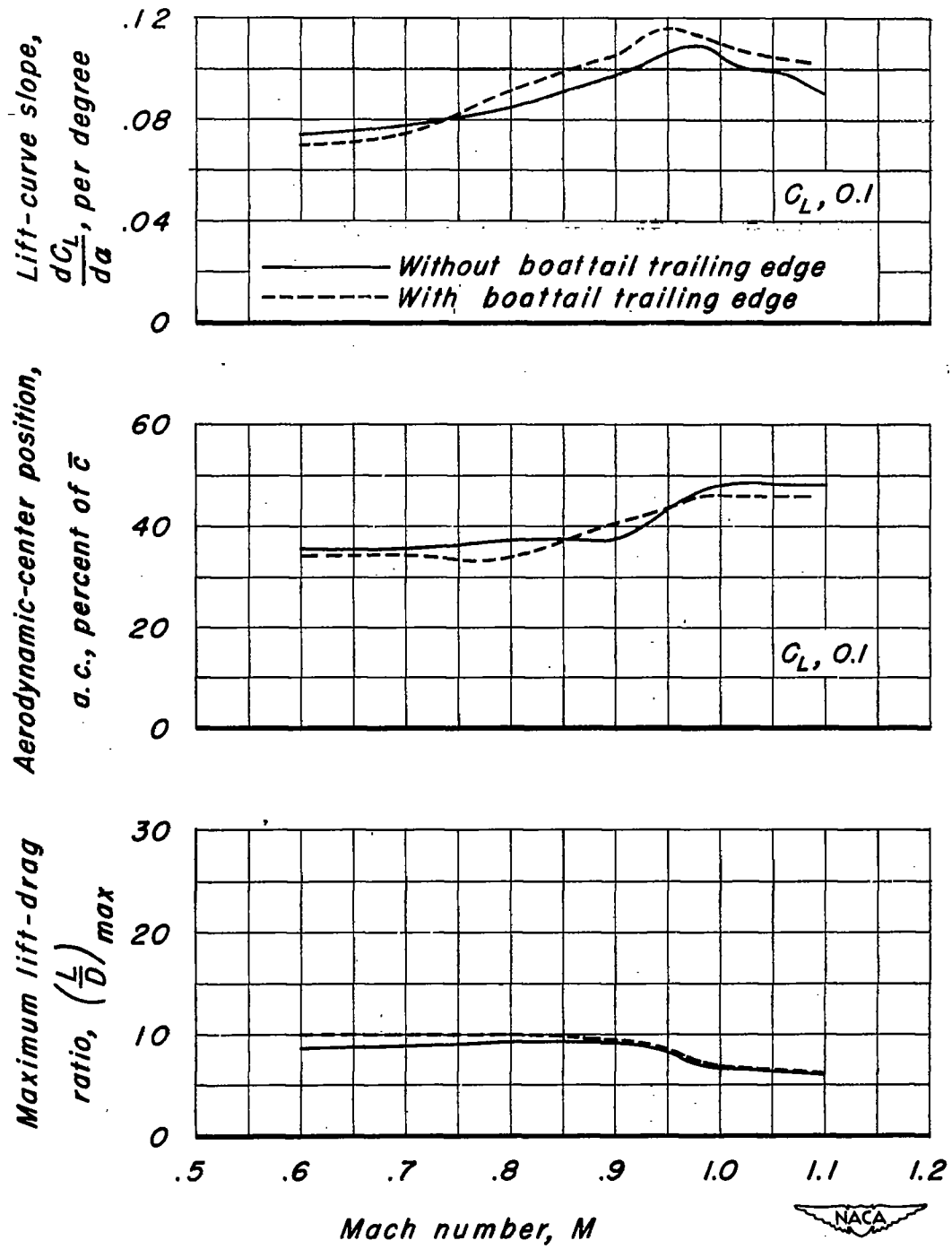

Figure 17.–Variation of aerodynamic parameters with Mach number for blunt and boattailed trailing edges.

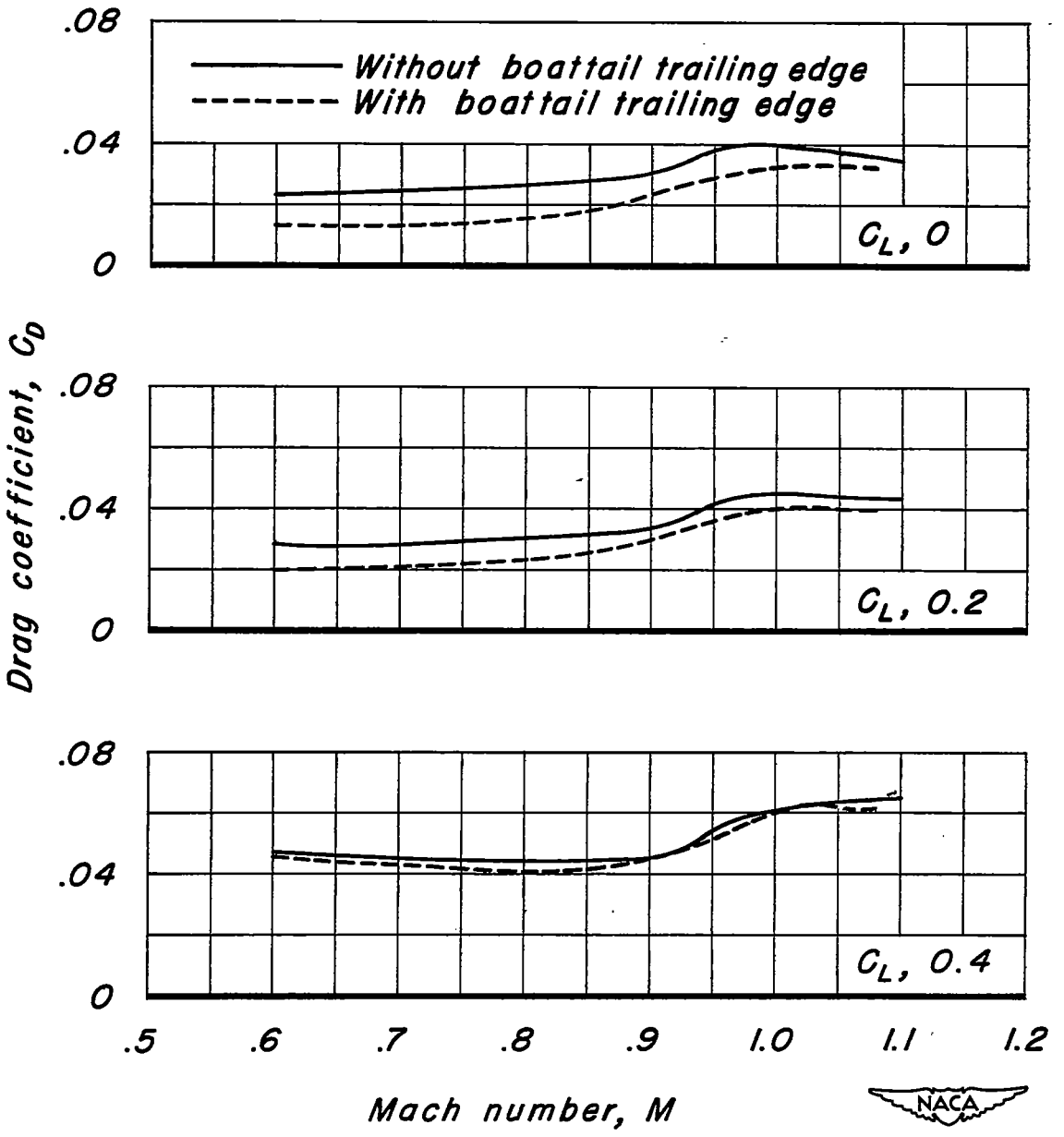

Figure 18.–Variation of drag coefficient with Mach number for blunt and boattailed trailing edges.

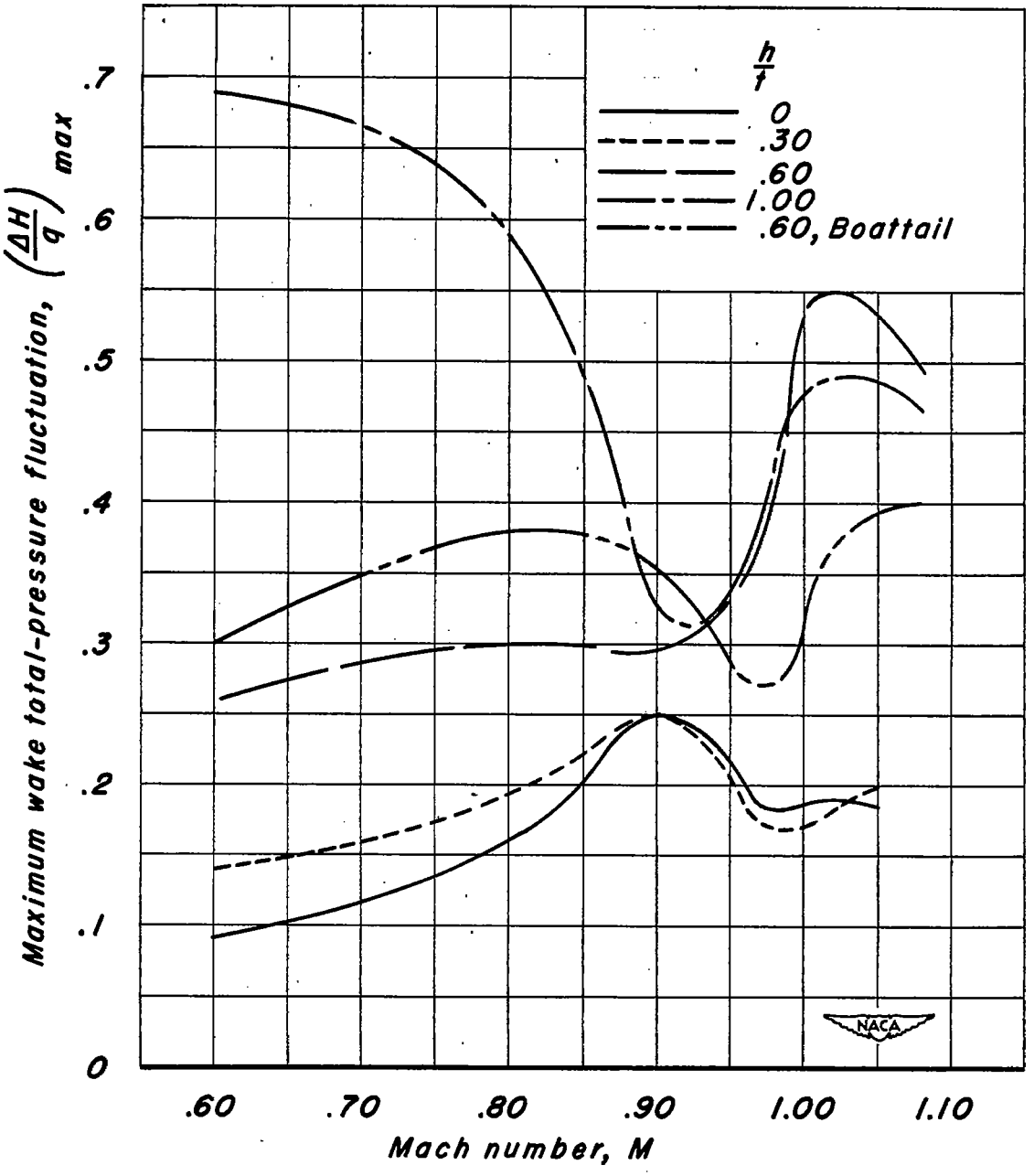

Figure 19.—Effect of Mach number on the wake maximum total-pressure fluctuation at various trailing edge thicknesses.

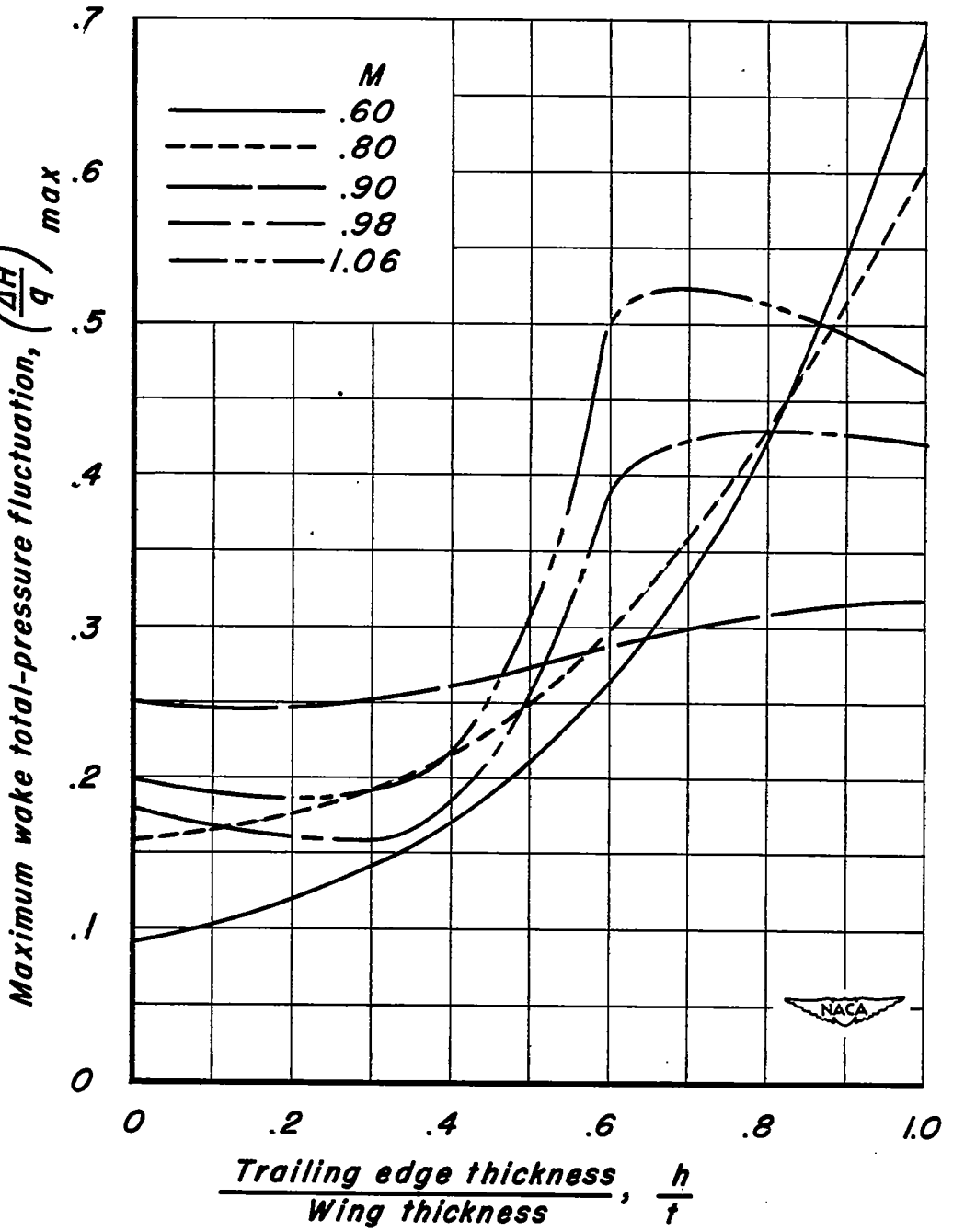

Figure 20.–Effect of trailing edge thickness on the maximum wake total-pressure fluctuation at several Mach numbers.

NACA-Langley - 12-11-51 - 325